NO_3 reactivity during a summer period in a temperate forest below and above the canopy

Patrick Dewald[1], Tobias Seubert[1], Simone T. Andersen[1], Gunther N. T. E. Türk[1], Jan Schuladen[1], Max R. McGillen[2], Cyrielle Denjean[3], Jean-Claude Etienne[3], Olivier Garrouste[3], Marina Jamar[4], Sergio Harb[5], Manuela Cirtog[5], Vincent Michoud[6], Mathieu Cazaunau[5], Antonin Bergé[5], Christopher Cantrell[5], Sebastien Dusanter[4], Bénédicte Picquet-Varrault[5], Alexandre Kukui[7], Chaoyang Xue[1,7], Abdelwahid Mellouki[2,8], Jos Lelieveld[1], and John N. Crowley[1]

[1]Atmospheric Chemistry Department, Max Planck Institute for Chemistry, 55128 Mainz, Germany
[2]Institut de Combustion, Aérothermique, Réactivité Environnement (ICARE), CNRS, 1C Avenue de la Recherche Scientifique, CEDEX 2, 45071 Orléans, France
[3]CNRM, Université de Toulouse, Meteo-France, CNRS, Toulouse, France
[4]IMT Nord Europe, Institut Mines-Télécom, Université de Lille, Center for Energy and Environment, 59000 Lille, France
[5]Université Paris Est Créteil and Université de Paris Cité, CNRS, LISA, F-94010 Créteil, France
[6]Université Paris Cité and Université Paris Est Créteil, CNRS, LISA, F-75013 Paris, France
[7]Laboratoire de Physique et Chimie de l'Environnement et de l'Espace (LPC2E), CNRS, Orléans, France
[8]University Mohammed VI Polytechnic (UM6P), Lot 660, Hay Moulay Rachid Ben Guerir, 43150, Morocco

Correspondence to: John N. Crowley (john.crowley@mpic.de)

Abstract. We present direct measurements of BVOC-induced nitrate radical (NO_3) reactivity (k^{VOC}) through the diel cycle in the suburban, temperate forest of Rambouillet near Paris (France). The data were obtained in a six-week summer period in 2022 as part of the ACROSS campaign (Atmospheric ChemistRy Of the Suburban foreSt). k^{VOC} was measured in a small (700 m^2) clearing mainly at a height of 5.5 m above ground level, but also at 40 m (for 5 days/nights). At nighttime, mean values (and 25th-75th percentile ranges) of k_{night}^{VOC}(5.5 m) = ($0.24^{+0.32}_{-0.06}$~~0.24 ± 0.27~~) s^{-1} and k_{night}^{VOC}(40 m) = ($0.016^{+0.018}_{-0.007}$~~0.016 ± 0.007~~) s^{-1} indicate a significant vertical gradient and low NO_3 reactivity above the canopy, whereas k_{night}^{VOC}(5.5 m) showed peak values of up to 2 s^{-1} close to the ground. The strong vertical gradient in NO_3 reactivity could be confirmed by measurements between 0 and 24 m on one particular night characterised by a strong temperature inversion, and is a result of the decoupling of air masses aloft from the ground- and canopy-level sources of BVOCs (and NO). No strong vertical gradient was observed in the mean daytime NO_3 reactivity with k_{day}^{VOC}(5.5 m) = (0.12 ± 0.04) s^{-1} for the entire campaign and k_{day}^{VOC}(40 m) = (0.07 ± 0.02) s^{-1} during the 5-day period.

Within the clearing, the fractional contribution of VOCs to the total NO_3 loss rate coefficient (~~L^{NO_3}~~ k^{tot}, determined by photolysis, reaction with NO and VOCs) was 80-90 % during the night and ~50 % during the day. In terms of chemical losses of α-pinene below canopy height in the clearing, we find that at nighttime OH and O_3 dominate with NO_3 contributing "only" 17 %, which decreases further to 8.5 % during the day. Based on measured OH, O_3 and calculated NO_3 concentrations, the chemical lifetime of BVOCs at noon is about one hour and is likely to be longer than timescales of transport out of the canopy

(typically in the order of minutes), thus significantly reducing the importance of daytime, in-canopy processing. Clearly, in forested regions where sufficient NO_X is available, the role of NO_3 and OH as initiators of BVOC oxidation are not strictly limited to the night and to the day, respectively, as often implied in e.g. atmospheric chemistry text-books.

1 Introduction

Forests emit great quantities (~ 1000 Tg yr^{-1}) of a variety of biogenic volatile organic compounds (BVOCs) such as isoprene and monoterpenes into the atmosphere (Guenther et al., 2012; Hakola et al., 2012; Vermeuel et al., 2023). The transport of combustion-related emissions from urban and industrialised regions results in the presence of NO_X (the sum of nitric oxide, NO and nitrogen dioxide, NO_2) in forested regions, as does microbial activity in soils (Ludwig et al., 2001; Barger et al., 2005; Pilegaard, 2013). An important step in photochemical ozone (O_3) generation is the oxidation of VOCs, which may be initiated by hydroxyl (OH) and nitrate radicals (NO_3) or O_3 itself (Geyer et al., 2001; Lelieveld et al., 2008; Peräkylä et al., 2014). The interaction of largely anthropogenic NO_X with BVOCs is thus a key component of tropospheric ozone production in many regions (Pusede et al., 2015). Here we focus on NO_3, which is formed from the reaction between NO_2 (e.g. from R1) and O_3 (R2) and is in a thermal equilibrium with NO_2 and dinitrogen pentoxide (N_2O_5, R3 and R4) (Wayne et al., 1991).

$NO + O_3 \rightarrow NO_2 + O_2$ (R1)

$NO_2 + O_3 \rightarrow NO_3 + O_2$ (R2)

$NO_3 + NO_2 + M \rightarrow N_2O_5 + M$ (R3)

$N_2O_5 + M \rightarrow NO_3 + NO_2 + M$ (R4)

In the troposphere, NO_3 reacts efficiently with NO to re-form NO_2 (R5), reacts with unsaturated VOCs (R6) and is photolysed rapidly with a lifetime that is often only a few seconds (R7a and R7b) (Finlayson-Pitts and Pitts, 2000). NO is reduced in concentration at night owing to its reaction with O_3 and since both NO and sunlight drastically reduce the lifetime of NO_3, the latter is often thought of as a "nighttime only" oxidant (Wayne et al., 1991; Platt and Heintz, 1994; Martinez et al., 2000; Brown and Stutz, 2012). Note that, in some environments, direct heterogeneous losses of NO_3 can also be important as can indirect losses via N_2O_5 uptake (Saathoff et al., 2001; Bertram and Thornton, 2009; Phillips et al., 2016).

$NO_3 + NO \rightarrow 2\ NO_2$ (R5)

$NO_3 + VOC\ (+ O_2) \rightarrow\rightarrow$ products (e.g. $RONO_2$, HNO_3) (R6)

$NO_3 + h\nu \rightarrow NO + O_2$ (R7a)

$NO_3 + h\nu \rightarrow NO_2 + O$ (R7b)

While both the reaction with NO (R5) and photolysis (R7) ~~regenerate NO_2 and thus~~ recycle either NO or NO_2~~NO_X~~, reactions between NO_3 and VOCs result in a variety of gas-phase products including organic nitrates ($RONO_2$) and nitric acid (HNO_3) (Hallquist et al., 1999; Ayres et al., 2015; Ng et al., 2017) which may be lost by deposition and/or transferred to the condensed phase, forming e.g. secondary organic aerosols (SOA) (Bates et al., 2022; Day et al., 2022; DeVault et al., 2022). The interaction of NO_3 with BVOCs can represent an efficient process for the removal of NO_X from the gas phase and a mechanism

Formatiert: Tiefgestellt

for SOA generation (Fry et al., 2014; Romer Present et al., 2020), making the fractional contribution of R6 to the overall loss rate of NO_3 of particular interest.

As unsaturated BVOCs such as isoprene and monoterpenes are often present at parts per billion by volume (ppbv) levels in the forest (Kesselmeier and Staudt, 1999; Hakola et al., 2009) the local NO_3 lifetimes are typically short not only during the day, but also at night (McLaren et al., 2004; Liebmann et al., 2018a; Liebmann et al., 2018b). NO_3 mixing ratios are often below 1 part per trillion by volume (pptv), making its detection in highly reactive air masses very challenging (Liebmann et al., 2018a). Measuring the NO_3 reactivity (together with NO_2 and O_3 to calculate the NO_3 production rate) provides a means to assess the atmospheric fate of the nitrate radical even when its mixing ratio is too low (< 0.5 pptv) to be detected (Dewald et al., 2022).

There are also meteorological effects that induce differences in the fate of NO_3 during the day and night. While daytime insolation at ground level can result in efficient (turbulent) mixing of the boundary layer, the radiative cooling of the ground at lower temperatures at night means that the nocturnal boundary layer can be highly stratified (Stull, 1988). This results in strong gradients in the mixing ratios of e.g. BVOCs (Fish et al., 1999) and the below-canopy reactivity of NO_3 can be very different to that above (Mogensen et al., 2015; Liebmann et al., 2018a). To date, NO_3 vertical profiles are available for high altitudes (i.e. above the boundary layer) in non-forested environments (Smith et al., 1993; von Friedeburg et al., 2002; Stutz et al., 2004; Brown et al., 2007a; Yan et al., 2021), yet highly-resolved vertical profiles of NO_3 (or its reactivity) for low altitudes at nighttime are sparse (Brown et al., 2007b; Liebmann et al., 2018a).

In this study, we present and analyse nighttime and daytime NO_3 reactivity measurements above and below the canopy in a temperate forest ca. 50 km from Paris (France) during the summer of 2022 as part of the ACROSS campaign (Atmospheric ChemistRy Of the Suburban foreSt) (Cantrell and Michoud, 2022).

2 Experimental

2.1 Site description and meteorology

The ACROSS campaign took place from mid-June until the end of July 2022 at a clearing (ca. 700 m^2) in the suburban forest of Rambouillet in France (N48.687, E1.704). Rambouillet forest covers an area of about 150 km^2 and is located about 50 km to the south-west of Paris. The surrounding trees are mainly oaks (~68 %) and pine (up to 25 %) (Marchant et al., 2017), with an average height of ~25 m. Daytime maximum temperatures during ACROSS were ~~between~~ ~20–40 °C (Fig.1, panel b), while nighttime temperatures decreased to 10–25 °C, often with a significant (positive) gradient in height that started to develop in the late afternoon when tree-induced shadowing of the ground led to radiative cooling (Andersen et al, 2024).

48h-back trajectories show that air originated from the Atlantic Ocean between June 25 and July 2, whereas air passed predominantly over industrialized regions including Paris, the UK, Benelux states and the Ruhr area from July 2 to July 18 (Andersen et al., 2024). Local wind directions and speeds are shown as a wind-rose in the Supplement (Fig. S1).

The clearing housed several instrumented containers and also a tower, which enabled measurements at 40 m to be made, either via instruments located at the top of the tower or via sampling from a gas-manifold attached to a high-flow inlet at the top of the tower.

2.2 NO_3 reactivity

The flow-tube cavity-ring-down spectrometer (FT-CRDS, Liebmann et al. (2017)) used to quantify NO_3 reactivity ~~(k^{VOC})~~ was installed in the MPIC container and sampled mainly from the centre of a high volume-flow (10000 standard L min^{-1}, SLPM) stainless steel tube (Ø = 15 cm) the top of which was at 5.5 m above ground level. We present measurements of k^{VOC} , which is defined as the VOC-induced pseudo first-order NO_3 loss rate coefficient (in units of s^{-1}) and is equal to $\Sigma k_i[VOC]_i$, with $[VOC]_i$ and k_i being the VOC concentrations and the corresponding rate coefficient for R6, respectively. The FT-CRDS was connected to the high-flow inlet with a 1.5 m long piece of ¼ inch outer diameter (OD) PFA tubing (overall residence time of 0.4 s) equipped with a Teflon membrane filter (2 µm pore, 47 mm diameter, Pall Corp.) to prevent particles entering the cavity. The filter was replaced every three days. From July 18, the NO_3 reactivity setup sampled air alternately from the high-flow inlet and from the manifold taking air from 40 m. The instrument was attached to the manifold with ca. 20 m ¼ inch PFA tubing (ca. 5 s residence time).

NO_3 was generated by mixing 3–5 standard cm^3 min^{-1} (sccm) of NO (1 part per million by volume (ppmv) in N_2, Air Liquide) with O_3 in a thermostated (30 °C), Teflon-coated (FEPD-121, Chemours) reactor (ca. 5 min residence time) at a pressure of 1100 Torr. O_3 was generated by the 185 nm photolysis of O_2 in a flow of 400 sccm dry synthetic air, which was provided from a commercial zero-air generator (CAP-180, Fuhr GmbH). In order to convert the resultant N_2O_5 quantitatively to NO_3 (R4), the flow was heated to 140 °C in ca. 15 cm of ¼ inch OD PFA tubing. The flow containing NO_3 was then mixed with 2.8 SLPM of either synthetic air (to define zero reactivity) or ambient air within a ¼ inch PFA T-piece and directed to the FEP-coated, darkened and thermostated (20°C) flow-tube where NO_3 had 11 s to react. NO_3 surviving the reactor was quantified on-line by cavity-ring-down spectroscopy at 662 nm. Zeroing ("baseline measurement") was achieved by adding an excess of NO (3 sccm of 100 ppmv in N_2, Air Liquide) to titrate NO_3 (R5). In synthetic air, the NO_3 mixing ratios were typically in the range of 30–50 pptv. As the presence of NO_3 and N_2O_5 in ambient air would bias the measurement, at nighttime the air was sampled through a 2 L glass flask (heated to 35 °C , ~~ca.~~ 40 s residence time) ~~heated to 35 °C~~ to ensure that ambient N_2O_5 is converted to NO_3. All radicals including NO_3, OH, RO_2 and HO_2 are lost on the glass walls and thus prevented from reaching the flowtube. From July 18, air was sampled through the glass flask throughout the diel cycle. No difference in k^{VOC} was observed directly after switching between "daytime mode" (no flask) and "nighttime mode" (sampling through flask), indicating that no compounds significantly contributing to k^{VOC} are lost in the glass flask. Accurate quantification of NO_3 reactivity requires that the synthetic air is humidified to ambient level (monitored with a commercial sensor, IST, HYT393), which was achieved with a permeation tube (MH-070-24F-4, PermaPure LLC) filled with de-ionized water (LiChrosolv, Merck GmbH). Dynamic dilution of ambient air with synthetic air extended the dynamic range of the instrument to NO_3 reactivities of up to ca. 2.1 s^{-1}. Since reactions R1 to R5 and wall losses (0.001 s^{-1}) take place in addition to the reaction of

Formatiert: Schriftart: Kursiv
Formatiert: Hochgestellt
Formatiert: Schriftart: Kursiv
Formatiert: Hochgestellt

interest (R6), a numerical simulation procedure was used to separate contributions of NO_X in the flowtube and thus extract the NO_3 reactivity towards VOCs as detailed in Liebmann et al. (2017). When sampling through the glass flask, ambient NO mixing ratios used for the simulation were corrected for the impact of R1 with correction factors between 1 and 40 %.

The uncertainty in k^{VOC} is determined by the stability of the NO_3 source, the cavity stability (i.e. noise level and baseline stability) and by the numerical simulation corrections. The uncertainty induced by the simulation is dependent on the ratio between NO_2 and k^{VOC} (Liebmann et al., 2017). During the campaign source and cavity stability, numerical simulation and uncertainties in the NO correction (impact of R5) contributed on average ca. 11, 9 and 26 % to the average overall uncertainty of ca. 30 %. The limit of detection (LOD) is derived from the variability (two standard deviations, 2σ) in consecutive baselines and NO_3 source measurements and was on average 0.006 s^{-1} during this campaign. In this manuscript we index the NO_3 reactivity according to the following scheme: k^{VOC}_{night}(5.5 m), k^{VOC}_{day}(5.5 m), k^{VOC}_{night}(40 m) and k^{VOC}_{day}(40 m) which are the measured reactivities towards VOCs during the day/night at the two different heights. Note that reactivity measurements at 40 m was limited to the last 5 days of the campaign. We also refer to ~~k^{totNO_3}~~ which is the total NO_3 loss term including reaction with NO and photolysis as well as reaction with VOCs.

2.3 NO, NO_2 and O_3

NO_2 mixing ratios at 5.5 m were measured by sampling via 1.5 m ¼ inch (OD) PFA tubing and a membrane filter (2 µm pore, 47 mm diameter, Pall Corp.) through the second (405 nm) cavity of the NO_3 reactivity instrument (Liebmann et al., 2018b). The instrument's LOD was 87 pptv (2σ, 4 s) and the measurement was associated with a total uncertainty of 7 %. On top of the tower (40 m), NO_2 was measured via a cavity attenuated phase shift (CAPS) setup (precision of 6 %, LOD of 40 pptv) which was zeroed on an hourly basis.

NO was measured using a commercial instrument based on chemiluminescence detection (Ecophysics, CLD 780 TR, LOD of 10 pptv for 1 min averaging time) which was installed in a container ca. 17 m distance from the MPIC container and sampled at a height of 3.2 m above the ground. The NO mixing ratios were corrected for a change in sensitivity during the campaign (Andersen et al., 2024). Measurement of NO at 40 m height was carried out using another CLD (Teledyne, T200UP) that sampled from the tower-manifold. This measurement was corrected for losses from R1, with corrections ranging from 1–28 %. The instrument's LOD was 30 pptv and its total uncertainty was 3.2 %.

A commercial ozone monitor (2B Technologies, model 205) based on UV absorption was installed in the MPIC container and measured ozone mixing ratios at 5.5 m height with an LOD of 2 ppbv and an associated uncertainty of 5 %. O_3 from top of the tower was quantified with means of a second ozone monitor with an LOD of 2.5 ppbv (HORIBA, APOA370).

2.4 Photolysis frequencies~~rates~~ and temperatures

Actinic flux was measured on top of the tower (41 m) as well as above the roof of the MPIC container (5 m), in both cases using spectral radiometers (Metcon GmbH). Actinic fluxes were converted to photolysis frequencies~~rates~~ of NO_3 and of other

compounds using IUPAC- and NASA-evaluated absorption cross sections (Burkholder et al., 2016; IUPAC, 2024)~~–~~. Commercial temperature sensors (Atexis PT1000 and Thermoset PT100) monitored ambient air temperature simultaneously at 5 m, 13 m, 21 m and 41 m.

3 Results and discussion

An overview of the measurements relevant for analysis of NO_3 reactivity is given in Fig. 1 where data obtained at 5.5 m (orange) and 40 m above ground level (blue) are plotted.

The VOC-induced NO_3 reactivity at a height of 5.5 m (k^{VOC}(5.5 m), panel f, orange triangles~~dots~~) was generally high with values between ~ 0.1 and 0.5 s^{-1} and also highly variable with nighttime peak values of up to 2 s^{-1}. In contrast, k^{VOC}_{night}(40 m) was often close to or below the LOD (≤ 0.006 s^{-1}) when sampling from top of the tower between July 18 – July 23 (panel f, blue ~~dots~~circles).

NO mixing ratios (panel e) at 3.2 m a.g.l. (orange circles~~dots~~) were on average between 0.1 and 0.3 ppbv, but occasionally peaked at 1–4 ppbv mostly in the morning during the continental phase. As detailed in Andersen et al. (2024), nighttime NO mixing ratios were close to or below the LOD when sampling air masses which, according to two-day back trajectories, were largely of continental origin (July 2 – July 18). In contrast, up to several ppbv of NO were observed at night during a period dominated by air with its origin over the Atlantic (June 26 – July 2) when O_3 levels (at 5.5 m) were below the LOD (panel c). NO_2 mixing ratios (panel d) were similar at both heights and, in the absence of anthropogenic influence, mostly between 0.5 and 2 ppbv.

The large diel variation in O_3 mixing ratios at 5.5 m (40–80 ppbv during the day and as low as zero at nighttime, panel c) results from its net daytime photochemical production through reactions involving OH, NO_X and VOCs (Crutzen and Lelieveld, 2001) and its nocturnal losses via reactions (e.g. with NO and BVOC) and deposition. Nocturnal O_3 mixing ratios at 40 m (20–40 ppbv) are higher than at 5.5 m (0–20 ppbv) and its diel cycle at 40 m is weaker than at 5.5 m. This results from a combination of removal processes of O_3 at lower levels (reaction with NO released from soil, reaction with unsaturated, biogenic VOCs released from vegetation and deposition to soil and foliar surfaces) and weak vertical mixing at nighttime (Andersen et al., 2024).

3.1 k^{VOC}: Variability and controlling factors close to the ground

At a height of 5.5 m, k^{VOC} shows large variability across the diel cycle and also from night-to-night (Fig. 1, panel f), which are driven by variability in emissions of reactive BVOCs and in the height of the nocturnal boundary layer (NBL). In Fig. 2, k^{VOC}(5.5 m) is plotted together with the difference in temperature (ΔT) measured at 5 and 41 m where ΔT = T(5 m) – T(41 m) and shows that the largest values of k^{VOC}_{night}(5.5 m) occur on nights when a temperature inversion (ΔT < 0 K) evolves. The impact of temperature inversion on NO_3 reactivity at 5.5 m is illustrated by comparing a night with no temperature inversion

(July 24 – July 25, period A) to a night with moderate temperature inversion (30 June – 1 July, period B). In the absence of a temperature inversion we see a roughly constant value < 0.1 s^{-1} for k^{VOC}(5.5 m) through the diel cycle (period A in the inset to Fig. 2). In contrast, when a temperature inversion developed (period B in the inset to Fig. 2), k^{VOC}(5.5 m) was relatively low (< 0.1 s^{-1}) until ca. 19:30 UTC. Over the next 2 hours, it gradually increased to reach peak values as large as 0.4 s^{-1}, which were associated with larger variability. Over the same period O_3 levels decreased from ~ 30–40 ppbv to < 10 ppbv, which has been rationalised in terms of suppression of entrainment of above-canopy air (with higher levels of O_3) into air masses close to the ground during temperature inversions (Andersen et al., 2024). The temperature inversion and associated reduction in vertical mixing impedes upward transport of both NO (emitted from the soil) and BVOCs (emitted from vegetation) so that both may accumulate within and below the canopy after sunset. The association of high values of k^{VOC}(5.5 m) with low values of O_3 during nighttime temperature inversions has previously been reported for the boreal forest (Liebmann et al., 2018a). In addition, elevated NO_3 reactivity at night is also aided by the fact that the nocturnal mixing ratios of O_3 and OH are diminished due to deposition and/or lack of photochemistry, so that the lifetime and mixing ratios of monoterpenes increase (see section 3.6).

The hypothesis that temperature inversions partially drive the observed NO_3 reactivity within the canopy is reinforced by close inspection of the temperature profiles in period B in the inset to Fig. 2. At 18:00 UTC, no gradient in temperature (16.5 °C) between 5 and 41 m was observed. At 20:30 UTC, a positive gradient in temperature was observed at heights > 20 m, becoming more distinct at 22:00 UTC. Under these conditions, vertical mixing from ground level to above-canopy-levels (ca. 20 m) is suppressed, whereas some mixing may still take place between 5 and 13 m where no temperature difference was observed. Weak (but non-zero) vertical mixing at the lower levels may be the cause of the high variability in k^{VOC}_{night}(5.5 m) whereby instabilities in the stratification at lower levels of the NBL allow sampling (at 5.5 m) of air with different (variable) time spent at lower/higher levels and thus with highly variable reactivity. The resulting high variability in NO_3 mixing ratios has been documented for NO_3 measurements made close to the ground (Brown et al., 2003; Crowley et al., 2010).

In forests, the most abundant BVOCs are typically isoprene and monoterpenes (Hakola et al., 2012; Vermeuel et al., 2023). Since the corresponding rate coefficients for the reaction of NO_3 with monoterpenes are up to two orders of magnitude larger than that of isoprene (IUPAC, 2024), monoterpenes are expected to be the main contributor to k^{VOC} during the ACROSS campaign. Relative monoterpene emission factors are temperature-dependent and described by exp(β(T-2~~7~~97 K)) with β = 0.1 K^{-1} in forested environments (Guenther et al., 1993), resulting in a strong seasonal variation (Hakola et al., 2006; Vermeuel et al., 2023). As a consequence, correlations between air temperature and VOC mixing ratios and OH reactivity have been reported (Kalogridis et al., 2014; Pfannerstill et al., 2021). Figure 3a shows that, during the day (black~~green~~ data points), with temperatures varying from 297 to 311 K, an increase in k^{VOC}(5.5 m) is observed. The inset contains daytime values measured between 10:00 and 14:00 UTC against air temperature and a linear regression suggests a fair correlation between the two (Pearson correlation coefficient r = 0.66). T~~t~~he expected factor of ~4 increase in the emission rate over this range as reported in Guenther et al. (1993) is much larger than the observed change in k^{VOC}(5.5 m). This is however expected as the daytime

concentrations of monoterpenes (MTs) will be determined not only by emission rates but also by their lifetime, which, in the clearing, will be reduced by reactions with daytime oxidants such as the OH and O_3 and (possibly more importantly) transport out of the canopy (Bohn, 2006). At nighttime (blue and red~~orange~~ dots in Fig. 3a), there is no clear correlation between k^{VOC}(5.5 m) and temperature, although the highest values of k^{VOC}(5.5 m) are generally observed at lower temperatures. A plot of k^{VOC}_{night}(5.5 m) versus ΔT and coloured according to the temperature at 5 m (Fig. 3b) reveals that higher NO_3 reactivity is accompanied by large (negative) values of ΔT. The maximum value of k^{VOC}_{night}(5.5 m) ≈ 2 s^{-1} was observed when a strong temperature inversion (ΔT < –6 K) coincided with a high nocturnal air temperature. During cooler nights (T(5 m) < 12 °C), k^{VOC}(5.5 m) was < 0.5 s^{-1} even during periods with very strong temperature inversions. Our analysis thus shows that while temperature is an important factor influencing NO_3 reactivity at 5.5 m through enhanced rates of emission of BVOCs, the effect (at least at sub-canopy levels) is greatly amplified by temperature inversions which favour accumulation of MTs in a shallow boundary layer close to the surface. In an upcoming publication we use monoterpene measurements to analyse NO_3 (and N_2O_5) mixing ratios and lifetimes at both 5.5 and 40 m heights during ACROSS and draw comparison between directly measured NO_3 reactivity and that attributed to various BVOC.

Formatiert: Schriftfarbe: Blau

3.2 Nitrate radical lifetime within and above the canopy

For the last five days of the ACROSS campaign (July 18 – July 23), the NO_3 reactivity was measured at a height of 40 m every even hour, with data obtained at 5.5 m every odd hour. The corresponding time-series of this measurement with a discussion of the vertical gradients observed during this period is appended in the Supplement (S2). With the data from this period, we could derive the total (chemical) loss rate coefficient of NO_3 not only at 5.5 m but also at 40 m, which is given by

$$~~L~~k^{\mathrm{tot}~~NO_3~~} \approx k^{\mathrm{VOC}} + J^{~~NO_3~~}_{NO_3} + k_5[\mathrm{NO}] \quad (1)$$

where k^{VOC} is our directly measured VOC-induced loss, ~~J^{NO_3}~~J_{NO_3} = k_{7a} + k_{7b} is the NO_3 photolysis frequency~~loss rate coefficient~~ (Fig. 1, panel a) and k_5 is the rate coefficient (IUPAC, 2024) for the reaction between NO and NO_3. Equation (1) neglects NO_3 loss processes resulting from direct (and indirect) heterogeneous reactions of NO_3 (and N_2O_5) as well as reactions with HO_x and organic radicals, which, for the ACROSS environment, is justified in the Supplement (S3). The NO_3 lifetime $\tau^{~~NO_3~~}_{NO_3}$ is the inverse of the total NO_3 loss rate coefficient:

$$\tau^{~~NO_3~~}_{NO_3} = {}^{1}/_{~~L^{NO_3}~~k^{tot}} \quad (2)$$

Formatiert: Tiefgestellt

Formatiert: Tiefgestellt

We plot τ_{NO_3} ~~τ^{NO_3}~~ through the diel cycle (5.5 and 40 m) in Fig. 4. For calculating ~~L~~$k^{~~NO_3~~\mathrm{tot}}$(5.5 m), the whole campaign period (as in Fig. 1) was considered since data gaps in both NO and $J^{~~NO_3~~}_{NO_3}$ ~~e~~ close to the ground and on top of the tower reduced the availability of quasi-simultaneous values of k^{tot} ~~L^{NO_3}~~(5.5 m) and k^{tot} ~~L^{NO_3}~~(40 m) (see Supplement S4). At a height of 5.5 m, the nocturnal lifetime of NO_3 is 2–3 s and (counterintuitively) somewhat longer (4–5 s) during the day despite the photolysis of NO_3. At a height of 40 m, above the canopy, the daytime lifetime of NO_3 is close to 3–4 s, whereas at night it increases to

10–12 s. The similar lifetimes at both heights during the day imply a vertically well-mixed layer. On the other hand, the longer nocturnal lifetime at 40 m compared to 5.5 m can be attributed to decoupling from direct (ground-level and within canopy) sources of NO and BVOCs (see section 3.1). The longer nocturnal lifetime of NO_3 at 40 m enabled it to be detected on some nights of the campaign, whereas NO_3 measurements were, unlike N_2O_5, always below LOD close to the ground. A detailed analysis of the NO_3 (and N_2O_5) measurements will be presented in a future publication.

3.3 Fate of the nitrate radical within the canopy

A mean diel cycle of k^{VOC}(5.5 m) for the whole campaign is depicted in Fig. 5. The higher mean nighttime value (k^{VOC}_{night}(5.5 m) = $(0.24^{+0.32}_{-0.06})$ ~~(0.24 ± 0.27)~~ s^{-1} compared to, k^{VOC}_{day}(5.5 m) = (0.12 ± 0.04) s^{-1}) is a result of the accumulation of BVOCs in a shallow, sub canopy layer with reduced rates of canopy-venting owing to temperature inversions. The observation of a daytime minimum and nighttime maximum in k^{VOC}(5.5 m) is consistent with measurements in the boreal forest in Finland (Liebmann et al., 2018a) where terpene emissions dominated the fate of NO_3 and strong temperature-inversions were present at night. Values of k^{VOC} in the boreal forest in autumn were a factor of 2–3 lower than those we measured in the temperate forest during ACROSS, which is presumably related to the lower temperatures as well as other factors such as leaf area index, vegetation-type and availability of oxidizing agents which affect the abundance of monoterpenes.

The fractional contribution F^{VOC}, of the reaction of NO_3 with VOCs to its total loss rate coefficient k^{tot} ~~L^{NO_3}~~, is given by Eq. (3)

$$F^{VOC} = k^{VOC}/k^{tot} \quad (3)$$

and shown in Fig. 5. At night, F^{VOC} (grey shaded area, blue line) is ca. 0.7–0.8, with the remaining 20 to 30 % assigned to reaction with NO. During the day, while photolysis (20 %) and reaction with NO (30 %) gain in importance, VOCs still account for 50 % of the NO_3 reactivity. The large daytime contribution of k^{VOC} is partly related to the fact that actinic flux (and thus the ~~rate of~~ photolysis frequencies of NO_3) within the clearing at 5.5 m height is reduced compared to above canopy levels (Fig. 1, panel a). In addition, the photolysis frequency for NO_2 is also reduced, so that the distribution of NO_X between NO and NO_2 is shifted towards NO_2 and away from NO, resulting in a reduction in k_5[NO]. In order to assess the impact of this effect, we calculated F^{VOC} with above-canopy values of J_{NO_3} and NO. In this scenario, daytime F^{VOC} increases to 33 %, i.e. the reduction of photolysis frequencies increases F^{VOC} by a factor of 1.5. Liebmann et al. (2018a) reported a daytime average for F^{VOC} of only 20 % in a boreal forest. Despite the fact that both sites are similarly affected by low NO and high monoterpene levels, this value is still significantly lower than 33 %, which can be reconciled with lower daytime values of k^{VOC} in the boreal forest. The comparatively high daytime contribution of VOCs to NO_3 consumption below the canopy thus stems from both reduction in J_{NO_3} and higher values of k^{VOC}, latter most likely due to higher concentrations of monoterpenes than in the boreal forest. This observation is consistent with even higher daytime VOC contributions to NO_3 loss of >97 % ~~Low daytime NO_3 photolysis frequencies have been~~ reported for sunlit wildfire plumes by Decker et al. (2021) who reconciled their result with

Formatiert: Tiefgestellt
Formatiert: Tiefgestellt
Formatiert: Hochgestellt
Formatiert: Hochgestellt
Formatiert: Hochgestellt
Feldfunktion geändert
Formatiert: Schriftfarbe: Text 1
Formatiert: Hochgestellt
Formatiert: Schriftart: Kursiv
Formatiert: Hochgestellt
Formatiert: Tiefgestellt
Formatiert: Hochgestellt
Formatiert: Tiefgestellt

VOC mixing ratios that were sufficiently high to outcompete photolysis and NO. ~~to result in NO_3 serving as the major VOC oxidant in wildfire plumes.~~

-We note at this point, that the photolysis frequencies measured in the clearing will be substantially larger than in the non-cleared forest.

By comparing $J_{NO_3}^{NO_3}$(5.5 m) with values observed above the canopy in the early morning and afternoon when the integrating-dome of the spectral-radiometer experienced only diffuse sunlight, we observe a reduction in J_{NO_3} ~~J^{NO_3}~~ (5.5 m) by a factor > 10 (Supplement S5). A substantial reduction in in-forest actinic flux compared to in a clearing and above the canopy has been reported by Bohn (2006) for a temperate, deciduous forest, albeit of different tree type and density of foliage. As discussed by Bohn (2006), a reduction in NO_3 photolysis frequency implies that the relative importance of NO_3 (compared to OH and O_3) as a daytime oxidant in the forest canopy is even larger than that (~50 %) derived above. A caveat to this is that the formation of NO_3 requires the presence of O_3 and NO_2, both of which are likely to have substantial deposition terms in dense foliage in the non-cleared forest. We also recognise that, during the daytime, the in-canopy chemical-lifetimes of BVOCs ~~S~~ may be much longer (see section 3.6) than the average residence time with respect to canopy-outflow, so that most BVOC daytime oxidation may take place above the forest.

3.4 Fate of the nitrate radical above the canopy

In Fig. 6, we plot the diel cycle of k^{VOC}(40 m) which shows a daytime maximum and nighttime minimum, which is the opposite of that measured at 5.5 m (see Fig. 5) but is typical for measurement sites that are decoupled from near-ground emissions during the night (Crowley et al., 2011; Liebmann et al., 2018b; Dewald et al., 2022). The daytime mean value of k_{day}^{VOC}(40 m) = (0.07 ± 0.02) s^{-1} is similar to those measured at 5.5 m, which presumably results from vertical mixing that is rapid compared to chemical lifetimes of BVOCs and NO. In contrast, the average value (± 25th and 75th percentile, respectively) of k_{night}^{VOC}(40 m) = ($0.016^{+0.018}_{-0.007}$ ~~0.016 ± 0.007~~) s^{-1} is approximately one order of magnitude lower than k_{night}^{VOC}(5.5 m). Recall however, that due to its poor data coverage during the 5-day-period, k^{VOC}(5.5 m) from the whole campaign is used for this comparison.

The daytime, chemical, gas-phase NO_3 loss processes at 40 m (see pie chart in Fig. 6) also differ significantly from those at 5.5 m (see Fig. 5) with the contribution of BVOCs almost halved (25.5 %) in favour of both NO (48 %) and photolysis (26.5 %). Reaction with NO is thus the main daytime loss process for NO_3 at 40 m, which is a result of greater NO mixing ratios at this height during the 5-day-period. But even at night, NO mixing ratios during this period were still high enough (40-150 pptv) to compete with VOCs. In addition, some days between July 18 and July 23 were cloudy, which is why NO_3 loss via reaction with NO prevails even at a height of 40 m. A time series comparing $J_{NO_3}^{NO_3}$, k_5[NO] and ~~k^{totNO_3}~~ at both heights during this period is appended in the Supplement (S4).

3.5 Vertical gradient (0-24 m) in NO_3 reactivity

During the night from July 17 to July 18 (a night with a strong temperature inversion with ΔT between –4 and –6 K), gas-phase NO_3 reactivity (resulting from reaction with both BVOCs and NO), NO_2 and O_3 were measured at heights between 0 and 24 m above ground level in 4 m steps. Measurements of NO_2 and O_3 at 40 m during the same night are also plotted in Fig. ~~7 2 (period P)~~. As NO mixing ratios were not available at all heights, the NO_3 reactivity was not corrected for this and thus includes NO_3 removal via reaction with NO ($k^{NO} = k_5[NO]$), i.e. k^{VOC} becomes $k^{VOC~~+NO~~} + k^{NO}$. Between 20:00 and 00:00 UTC five profiles of $k^{VOC} + k^{NO}k^{~~VOC+NO~~}$ were measured, each taking < 20 min. The first profile was measured after an increase in k^{VOC}_{night}(5.5 m) which was associated with the onset of the temperature inversion. $k^{VOC} + k^{NO}k^{~~VOC+NO~~}$ (averaged over the 5 single profiles) is plotted versus height in Fig. 7c along with the data obtained at 40 m in the following nights (see section 3.2). The data reveal a strong trend in NO_3 reactivity with the highest values (0.34 s^{-1}) measured at ground level, where NO is expected to have a greater impact, gradually decreasing with height to a value of ca. 0.08 s^{-1} at 24 m. The data at 40 m (uncorrected for NO) are broadly consistent with this trend and, together with Fig. 6, imply that NO is the main contributor to NO_3 reactivity above canopy level. The gradient in NO_2 (Fig. 7b) shows no clear trend for heights below 24 m and is determined by its nighttime production (mainly the reaction between NO and O_3) which depends on the availability of NO and the availability of O_3 (which has a positive gradient). As modelled in Stutz et al. (2004), a negative nocturnal gradient in NO with height is expected, notably due to ~~low level~~ soil emission and reaction with O_3 (Andersen et al., 2024). In addition, NO_2 loss via deposition is expected to be more important at the lower levels. These processes appear to roughly counterbalance each other on this night, resulting in an almost constant mixing ratio between ground level and 24 m. This observation is consistent with those in Stutz et al. (2004), who could, if at all, only find very weak gradients. Fig. 7a also includes the vertical profiles of O_3 which increases from ca. 27 ppbv at ground-level to 58 ppbv at 40 m presumably a result of near-ground loss processes such as deposition and reaction with NO / BVOCs and lack of entrainment of O_3 from above the canopy, where higher mixing ratios were measured (Fig. 1, panel c) (Brown et al., 2007a). The measured vertical profiles of O_3 were much less distinct in Stutz et al. (2004), which contradicted their model calculations that suggested a monotonic increase within the first 100 m, broadly consistent with our case study.

3.6 Fractional contribution of NO_3 to BVOC oxidation below the canopy

Our results show that, within the canopy, the nitrate radical is lost by reactions with BVOCs not only during the night but also during the day. Here we calculate the fractional contribution of NO_3 to the oxidation of a dominant BVOC, α-pinene (Guenther et al., 2012; Liebmann et al., 2018a; Vermeuel et al., 2023). As detailed in Eq. (4) the overall ~~oxidation~~ loss rate coefficient for α-pinene ($k_{~~OH~~+\alpha\text{-pinene}}$) can be calculated from the concentrations of each oxidant (OH, NO_3 and O_3) and the corresponding rate coefficients $k_{x+\alpha\text{-pin}}$ of 5.3×10^{-11}, 6.2×10^{-12} and 9.6×10^{-17} cm^3 $molecule^{-1}$ s^{-1} for the reaction of OH, NO_3 and O_3 with α-pinene at 298 K, respectively (IUPAC, 2024).

Formatiert: Schriftfarbe: Blau
Formatiert: Schriftart: Kursiv
Formatiert: Tiefgestellt
Formatiert: Tiefgestellt
Formatiert: Tiefgestellt
Formatiert: Tiefgestellt

$$k_{\alpha-\text{pinene}}L^{\alpha-\text{pinene}} = k_{\text{OH}+\alpha-\text{pinene}}[\text{OH}] + k_{\text{O}_3+\alpha-\text{pinene}}[\text{O}_3] + k_{\text{NO}_3+\alpha-\text{pinene}}[\text{NO}_3]_{\text{ss}} \quad (4)$$

As measured NO_3 mixing ratios near ground-level were below the LOD of 2 pptv throughout the whole campaign, we have derived steady-state mixing ratios, $[NO_3]_{ss}$, from the ratio of production ($k_2[NO_2][O_3]$) and overall NO_3 loss rate coefficients~~s~~ kL^{totNO_3} (Eq. 1) (Heintz et al., 1996; Brown et al., 2003; McLaren et al., 2010; Crowley et al., 2011). Note that the OH measurements were carried out with a chemical ionization mass spectrometer (CIMS, Kukui et al. (2008), see Supplement S3) ca. 17 m apart from the MPIC container. Figure 8 (upper panel) depicts the campaign-averaged, median mixing ratios of OH, O_3 and NO_3 (steady-state) throughout the diel cycle. Nighttime, steady-state NO_3 mixing ratios were 0.1-0.2 pptv during late evening until midnight, decreasing to < 0.1 ppt between midnight and dawn.~~,~~ This~~which~~ is not only related to ~~,~~the reduced availability of O_3 but also to the increase in k^{VOC}, both of which were usually accompanied by temperature inversions.~~.~~ Remarkably, daytime NO_3 values were similar and occasionally even higher than nighttime values, emphasising the fact that photolysis was not the major daytime loss process for NO_3. As expected, OH mixing ratios were highest during the daytime (peak value of 0.14 pptv), but were ~~also present~~not zero at night (0.01–0.03 pptv). Nighttime OH is formed in the oxidation of terpenes by O_3 and in secondary reactions of RO_2 and HO_2 (formed in same process) with NO ~~reactions~~. Median O_3 mixing ratios reached ca. 44 ppbv during the day and continuously decreased to ca. 15 ppbv during the night and the early morning. The fractional contribution of each oxidant to $k_{\alpha-\text{pinene}}$ ~~$L^{\alpha-\text{pinene}}$~~ is presented as a median diel profile for the whole campaign in the lower panel of Fig. 8. Based on the above analysis, in the summertime forested environment probed during ACROSS, NO_3 contributed *only* ca. 17 % to the nighttime oxidation of α-pinene, a value that is exceeded by both OH (ca. 24 %) and O_3 (60 %). The daytime dominance of OH and O_3 (on average ca. 50 and 41.5 %, respectively) is expected, whilst, with a contribution of 8.5 % the diel- and campaign-averaged contribution of NO_3 is still significant, which is in agreement with recent publications (Schulze et al., 2017; Liebmann et al., 2018b; Mermet et al., 2021; Dewald et al., 2022) and model calculations showing that NO_3 oxidizes BVOCs below the canopy level during daytime in both coniferous and deciduous forests (Forkel et al., 2006; Fuentes et al., 2007). We further note that the oxidation of BVOCs by OH, O_3 and NO_3 results in greatly different products, so that in terms of formation of organic nitrates, NO_3-initiated oxidation can still dominate (Liebmann et al., 2019). A detailed analysis on the role of NO_3-initated organic nitrate formation will be presented in a further publication ~~describing~~ from the ACROSS campaign. Recall that the fractional contributions are highly dependent on the ratios between the rate coefficients of the oxidants and are thus different for other monoterpenes. As shown in the Supplement (S6), this is reflected in lower fractional contributions of NO_3 to the oxidation of β-pinene and limonene with values of 12.4 and 13.5 % at night and 4.4 and 6.2 % during the day.

Our analysis is not consistent with the generally accepted text-book paradigm that OH-initiated oxidation processes are predominant during the day and NO_3-initiated oxidation prevails at night. However, an important caveat to our analysis is the neglect of daytime transport (venting) of BVOCs out of the forest. If this proceeds at time-scales that are short compared to

Formatiert: Tiefgestellt

Formatiert: Schriftart: Kursiv

Formatiert: Hochgestellt

the chemical lifetime of BVOCs, then in-canopy oxidation will be of reduced importance compared to oxidation once BVOCs have been transported to ~~the~~ higher levels within the boundary layer and free troposphere (Bohn, 2006).

4 Conclusions and summary

During a field campaign in a peri-urban, temperate (oak and pine) forest in France during a summer period in 2022, the reactivity of the NO_3 radical towards VOCs was measured both within the canopy (height of 5.5 m), above the canopy (height of 40 m) and on one night at several heights between 0 and 24 m. NO_3 lifetimes were generally short (1–3 s) which were driven mainly by the abundance of BVOCs. Diel cycles of NO_3 at 5.5 m and 40 m were distinct, with the highest reactivity at 40 m occurring during the day and the highest reactivity at 5.5 m measured at nighttime. The highest nighttime reactivities were associated with high temperatures (driving the BVOC emissions) and with strong nighttime temperature inversions (preventing mixing of BVOCs and NO out of the nocturnal surface layer). At 5.5 m, BVOCs represented the dominant loss term for NO_3 both during the night (70–80 %) and during the day (~50 %), which is partially a result of reduced NO_3 (and NO_2) photolysis frequencies at sub-canopy heights. NO_3 reactivity decreased rapidly with height above the ground with nocturnal lifetimes (with respect to reaction with VOCs) of > 100 s at 40 m and as low as 2.5 s at ground-level. This gradient is driven largely by BVOC and NO emissions into a shallow, stratified near-surface layer under canopy height.

The conventional wisdom, that OH is a daytime oxidant and NO_3 a nighttime oxidant appears not to apply to forested regions with significant BVOC emissions where both NO_3 and OH have important roles throughout the diel cycle. Hence, NO_3-initiated organic nitrate formation could become significant during the day, whereas OH-initiated nocturnal chemistry would be enhanced in such environments.

Data Availability. All data can be found on https://across.aeris-data.fr/catalogue/.

Author contributions. PD analysed the data and wrote the original draft of the manuscript and, together with JNC, revised it. CC and VM were responsible for the campaign organization with contributions from individual group leads. All authors provided measurements and commented on the manuscript.

Competing Interests. At least one of the (co-)authors is a member of the editorial board of Atmospheric Chemistry and Physics.

Acknowledgements.

JC acknowledges Chemours for the provision of a FEPD-121 sample used to coat the flowtube and the Deutsche Forschungsgemeinschaft (project "MONOTONS", project number: 522970430). STA thanks the Alexander von Humboldt foundation for funding her stay at the MPIC. The ACROSS project has received funding from the French National Research Agency (ANR) under the investment program integrated into France 2030, with the reference ANR-17-MPGA-0002, and it

was supported by the French National program LEFE (Les Enveloppes Fluides et l'Environnement) of the CNRS/INSU (Centre National de la Recherche Scientifique/Institut National des Sciences de l'Univers). IMT Nord Europe acknowledges financial support from the CaPPA project, which is funded by the French National Research Agency (ANR) through the PIA (Programme d'Investissement d'Avenir) under contract ANR-11-LABX-0005-01, the Regional Council "Hauts-de-France" and the European Regional Development Fund (ERDF). Data from the ACROSS campaign are hosted by the French national centre for Atmospheric data and services AERIS. AK acknowledges financial support from the VOLTAIRE project (ANR-10-LABX-100-01) funded by ANR through the PIA (Programme d'Investissement d'Avenir). The scientific colour map "Berlin" (Crameri, 2023) is used in this study to prevent visual distortion of the data and exclusion of readers with colour-deficiencies (Crameri et al., 2020).

References

Andersen, S. T., McGillen, M. R., Xue, C., Seubert, T., Dewald, P., Türk, G. N. T. E., Schuladen, J., Denjean, C., Etienne, J. C., Garrouste, O., Jamar, M., Harb, S., Cirtog, M., Michoud, V., Cazaunau, M., Bergé, A., Cantrell, C., Dusanter, S., Picquet-Varrault, B., Kukui, A., Mellouki, A., Carpenter, L. J., Lelieveld, J., and Crowley, J. N.: Measurement report: Sources, sinks and lifetime of NOX in a sub-urban temperate forest at night, EGUsphere, 2024, 1-29, doi:10.5194/egusphere-2023-2848, 2024.

Ayres, B. R., Allen, H. M., Draper, D. C., Brown, S. S., Wild, R. J., Jimenez, J. L., Day, D. A., Campuzano-Jost, P., Hu, W., de Gouw, J., Koss, A., Cohen, R. C., Duffey, K. C., Romer, P., Baumann, K., Edgerton, E., Takahama, S., Thornton, J. A., Lee, B. H., Lopez-Hilfiker, F. D., Mohr, C., Wennberg, P. O., Nguyen, T. B., Teng, A., Goldstein, A. H., Olson, K., and Fry, J. L.: Organic nitrate aerosol formation via NO_3 + biogenic volatile organic compounds in the southeastern United States, Atmos. Chem. Phys., 15, 13377-13392, doi:10.5194/acp-15-13377-2015, 2015.

Barger, N. N., Belnap, J., Ojima, D. S., and Mosier, A.: NO gas loss from biologically crusted soils in Canyonlands National Park, Utah, Biogeochemistry, 75, 373-391, doi:10.1007/s10533-005-1378-9, 2005.

Bates, K. H., Burke, G. J. P., Cope, J. D., and Nguyen, T. B.: Secondary organic aerosol and organic nitrogen yields from the nitrate radical (NO_3) oxidation of alpha-pinene from various RO_2 fates, Atmos. Chem. Phys., 22, 1467-1482, doi:10.5194/acp-22-1467-2022, 2022.

Bertram, T. H., and Thornton, J. A.: Toward a general parameterization of N_2O_5 reactivity on aqueous particles: the competing effects of particle liquid water, nitrate and chloride, Atmos. Chem. Phys., 9, 8351-8363, doi:10.5194/acp-9-8351-2009, 2009.

Bohn, B.: Solar spectral actinic flux and photolysis frequency measurements in a deciduous forest, J. Geophys. Res.-Atmos., 111, D15303, doi:10.1029/2005JD006902, 2006.

Brown, S. S., Stark, H., Ryerson, T. B., Williams, E. J., Nicks, D. K., Trainer, M., Fehsenfeld, F. C., and Ravishankara, A. R.: Nitrogen oxides in the nocturnal boundary layer: Simultaneous in situ measurements of NO_3, N_2O_5, NO_2, NO, and O_3, J. Geophys. Res.-Atmos., 108, 4299, doi:10.1029/2002JD002917, 2003.

Brown, S. S., Dube, W. P., Osthoff, H. D., Stutz, J., Ryerson, T. B., Wollny, A. G., Brock, C. A., Warneke, C., De Gouw, J. A., Atlas, E., Neuman, J. A., Holloway, J. S., Lerner, B. M., Williams, E. J., Kuster, W. C., Goldan, P. D., Angevine, W. M., Trainer, M., Fehsenfeld, F. C., and Ravishankara, A. R.: Vertical profiles in NO_3 and N_2O_5 measured from an aircraft: Results

Formatiert: Englisch (Vereinigtes Königreich)

from the NOAA P-3 and surface platforms during the New England Air Quality Study 2004, J. Geophys. Res.-Atmos., 112, D22304, doi: 10.1029/2007jd008893, 2007a.

Brown, S. S., Dube, W. P., Osthoff, H. D., Wolfe, D. E., Angevine, W. M., and Ravishankara, A. R.: High resolution vertical distributions of NO_3 and N_2O_5 through the nocturnal boundary layer, Atmos. Chem. Phys., 7, 139-149, doi:10.5194/acp-7-139-2007, 2007b.

Brown, S. S., and Stutz, J.: Nighttime radical observations and chemistry, Chem. Soc. Rev., 41, 6405–6447, doi:10.1039/C2CS35181A, 2012.

Burkholder, J. B., Sander, S. P., Abbatt, J. , Barker, J. R, Huie, R. E., Kolb, C. E., Kurylo, M. J., Orkin, V. L., Wilmouth, D. M.., and Wine, P. H.: Chemical Kinetics and Photochemical Data for Use in Atmospheric Studies, Evaluation No. 18," JPL Publication 15-10, Jet Propulsion Laboratory, Pasadena: https://jpldataeval.jpl.nasa.gov, access: 23 July 2023, 2016.

Cantrell, C., and Michoud, V.: An Experiment to Study Atmospheric Oxidation Chemistry and Physics of Mixed Anthropogenic–Biogenic Air Masses in the Greater Paris Area, Bulletin of the American Meteorological Society, 103, 599-603, doi:10.1175/BAMS-D-21-0115.1, 2022.

Crameri, F., Shephard, G. E., and Heron, P. J.: The misuse of colour in science communication, Nat. Commun., 11, 5444, doi:10.1038/s41467-020-19160-7, 2020.

Crameri, F.: Scientific colour maps (8.0.1), Zenodo, doi:10.5281/zenodo.8409685, 2023.

Crowley, J. N., Schuster, G., Pouvesle, N., Parchatka, U., Fischer, H., Bonn, B., Bingemer, H., and Lelieveld, J.: Nocturnal nitrogen oxides at a rural mountain site in south-western Germany, Atmos. Chem. Phys., 10, 2795-2812, doi:10.5194/acp-10-2795-2010, 2010.

Crowley, J. N., Thieser, J., Tang, M. J., Schuster, G., Bozem, H., Hasaynali Beygi, Z., Fischer, H., Diesch, J.-M., Drewnick, F., Borrmann, S., Song, W., Yassaa, N., Williams, J., Pöhler, D., Platt, U., and Lelieveld, J.: Variable lifetimes and loss mechanisms for NO_3 and N_2O_5 during the DOMINO campaign: Contrast between marine, urban and continental air, Atmos. Chem. Phys., 11, 10863-10870, doi:10.5194/acp-11-10853-2011, 2011.

Crutzen, P. J., and Lelieveld, J.: Human impacts on atmospheric chemistry, Annu. Rev. Earth Planet. Sci., 29, 17-45, doi:10.1146/annurev.earth.29.1.17, 2001.

Day, D. A., Fry, J. L., Kang, H. G., Krechmer, J. E., Ayres, B. R., Keehan, N. I., Thompson, S. L., Hu, W. W., Campuzano-Jost, P., Schroder, J. C., Stark, H., DeVault, M. P., Ziemann, P. J., Zarzana, K. J., Wild, R. J., Dube, W. P., Brown, S. S., and Jimenez, J. L.: Secondary Organic Aerosol Mass Yields from NO_3 Oxidation of alpha-Pinene and Delta-Carene: Effect of RO_2 Radical Fate, J. Phys. Chem. A, doi:10.1021/acs.jpca.2c04419, 2022.

Decker, Z. C. J., Robinson, M. A., Barsanti, K. C., Bourgeois, I., Coggon, M. M., DiGangi, J. P., Diskin, G. S., Flocke, F. M., Franchin, A., Fredrickson, C. D., Gkatzelis, G. I., Hall, S. R., Halliday, H., Holmes, C. D., Huey, L. G., Lee, Y. R., Lindaas, J., Middlebrook, A. M., Montzka, D. D., Moore, R., Neuman, J. A., Nowak, J. B., Palm, B. B., Peischl, J., Piel, F., Rickly, P. S., Rollins, A. W., Ryerson, T. B., Schwantes, R. H., Sekimoto, K., Thornhill, L., Thornton, J. A., Tyndall, G. S., Ullmann, K., Van Rooy, P., Veres, P. R., Warneke, C., Washenfelder, R. A., Weinheimer, A. J., Wiggins, E., Winstead, E., Wisthaler, A., Womack, C., and Brown, S. S.: Nighttime and daytime dark oxidation chemistry in wildfire plumes: an observation and model analysis of FIREX-AQ aircraft data, Atmos. Chem. Phys., 21, 16293-16317, doi:10.5194/acp-21-16293-2021, 2021.

Feldfunktion geändert

Formatiert: Englisch (Vereinigtes Königreich)

Formatiert: Englisch (Vereinigtes Königreich)

DeVault, M. P., Ziola, A. C., and Ziemann, P. J.: Products and Mechanisms of Secondary Organic Aerosol Formation from the NO_3 Radical-Initiated Oxidation of Cyclic and Acyclic Monoterpenes, ACS Earth Space Chem., 6, 2076-2092, doi:10.1021/acsearthspacechem.2c00130, 2022.

Dewald, P., Nussbaumer, C. M., Schuladen, J., Ringsdorf, A., Edtbauer, A., Fischer, H., Williams, J., Lelieveld, J., and Crowley, J. N.: Fate of the nitrate radical at the summit of a semi-rural mountain site in Germany assessed with direct reactivity measurements, Atmos. Chem. Phys., 22, 7051-7069, doi:10.5194/acp-22-7051-2022, 2022.

Finlayson-Pitts, B. J., and Pitts, J. N.: CHAPTER 7 - Chemistry of Inorganic Nitrogen Compounds: Chemistry of the Upper and Lower Atmosphere, edited by: Finlayson-Pitts, B. J., and Pitts, J. N., Academic Press, San Diego, 264-293, 2000.

Fish, D. J., Shallcross, D. E., and Jones, R. L.: The vertical distribution of NO_3 in the atmospheric boundary layer, Atmos. Environ., 33, 687-691, doi:10.1016/S1352-2310(98)00332-X, 1999.

Forkel, R., Klemm, O., Graus, M., Rappenglück, B., Stockwell, W. R., Grabmer, W., Held, A., Hansel, A., and Steinbrecher, R.: Trace gas exchange and gas phase chemistry in a Norway spruce forest:: A study with a coupled 1-dimensional canopy atmospheric chemistry emission model, Atmos. Environ., 40, S28-S42, doi:10.1016/j.atmosenv.2005.11.070, 2006.

Fry, J. L., Draper, D. C., Barsanti, K. C., Smith, J. N., Ortega, J., Winkle, P. M., Lawler, M. J., Brown, S. S., Edwards, P. M., Cohen, R. C., and Lee, L.: Secondary Organic Aerosol Formation and Organic Nitrate Yield from NO_3 Oxidation of Biogenic Hydrocarbons, Environ. Sci. Technol., 48, 11944-11953, doi:10.1021/es502204x, 2014.

Fuentes, J. D., Wang, D., Bowling, D. R., Potosnak, M., Monson, R. K., Goliff, W. S., and Stockwell, W. R.: Biogenic hydrocarbon chemistry within and above a mixed deciduous forest, J. Atmos. Chem., 56, 165-185, doi:10.1175/1520-0477(2000)081<1537:BHITAB>2.3.CO;2, 2007.

Geyer, A., Alicke, B., Konrad, S., Schmitz, T., Stutz, J., and Platt, U.: Chemistry and oxidation capacity of the nitrate radical in the continental boundary layer near Berlin, J. Geophys. Res.-Atmos., 106, 8013-8025, doi:10.1029/2000jd900681, 2001.

Guenther, A. B., Zimmerman, P. R., Harley, P. C., Monson, R. K., and Fall, R.: Isoprene and Monoterpene Emission Rate Variability - Model Evaluations and Sensitivity Analyses, J. Geophys. Res.-Atmos., 98, 12609-12617, doi:10.1029/93jd00527, 1993.

Guenther, A. B., Jiang, X., Heald, C. L., Sakulyanontvittaya, T., Duhl, T., Emmons, L. K., and Wang, X.: The Model of Emissions of Gases and Aerosols from Nature version 2.1 (MEGAN2.1): an extended and updated framework for modeling biogenic emissions, Geosci. Model. Dev., 5, 1471-1492, doi:10.5194/gmd-5-1471-2012, 2012.

Hakola, H., Tarvainen, V., Back, J., Ranta, H., Bonn, B., Rinne, J., and Kulmala, M.: Seasonal variation of mono- and sesquiterpene emission rates of Scots pine, Biogeosciences, 3, 93-101, doi:10.5194/bg-3-93-2006, 2006.

Hakola, H., Hellén, H., Tarvainen, V., Bäck, J., Patokoski, J., and Rinne, J.: Annual variations of atmospheric VOC concentrations in a boreal forest, Boreal Env. Res., 14, 722-730, 2009.

Hakola, H., Hellén, H., Hemmilä, M., Rinne, J., and Kulmala, M.: In situ measurements of volatile organic compounds in a boreal forest, Atmos. Chem. Phys., 12, 11665-11678, doi:10.5194/acp-12-11665-2012, 2012.

Hallquist, M., Wangberg, I., Ljungstrom, E., Barnes, I., and Becker, K. H.: Aerosol and product yields from NO_3 radical-initiated oxidation of selected monoterpenes, Environ. Sci. Technol., 33, 553-559, doi:10.1021/es980292s, 1999.

Heintz, F., Platt, U., Flentje, H., and Dubois, R.: Long-term observation of nitrate radicals at the tor station, Kap Arkona (Rügen), J. Geophys. Res.-Atmos., 101, 22891-22910, doi:10.1029/96JD01549, 1996.

IUPAC: Task Group on Atmospheric Chemical Kinetic Data Evaluation, edited by: Ammann, M., Cox, R.A., Crowley, J.N., Herrmann, H., Jenkin, M.E., McNeill, V.F., Mellouki, A., Rossi, M. J., Troe, J. and Wallington, T. J.: https://iupac.aeris-data.fr/en/home-english/, access: 29 January, 2024.

Kalogridis, C., Gros, V., Sarda-Esteve, R., Langford, B., Loubet, B., Bonsang, B., Bonnaire, N., Nemitz, E., Genard, A. C., Boissard, C., Fernandez, C., Ormeño, E., Baisnée, D., Reiter, I., and Lathière, J.: Concentrations and fluxes of isoprene and oxygenated VOCs at a French Mediterranean oak forest, Atmos. Chem. Phys., 14, 10085-10102, doi:10.5194/acp-14-10085-2014, 2014.

Kesselmeier, J., and Staudt, M.: Biogenic volatile organic compounds (VOC): An overview on emission, physiology and ecology, J. Atmos. Chem., 33, 23-88, doi:10.1023/a:1006127516791, 1999.

Kukui, A., Ancellet, G., and Le Bras, G.: Chemical ionisation mass spectrometer for measurements of OH and Peroxy radical concentrations in moderately polluted atmospheres, J. Atmos. Chem., 61, 133-154, doi:10.1007/s10874-009-9130-9, 2008.

Lelieveld, J., Butler, T. M., Crowley, J. N., Dillon, T. J., Fischer, H., Ganzeveld, L., Harder, H., Lawrence, M. G., Martinez, M., Taraborrelli, D., and Williams, J.: Atmospheric oxidation capacity sustained by a tropical forest, Nature, 452, 737-740, doi:10.1038/nature06870, 2008.

Liebmann, J., Karu, E., Sobanski, N., Schuladen, J., Ehn, M., Schallhart, S., Quéléver, L., Hellen, H., Hakola, H., Hoffmann, T., Williams, J., Fischer, H., Lelieveld, J., and Crowley, J. N.: Direct measurement of NO_3 radical reactivity in a boreal forest, Atmos. Chem. Phys., 18, 3799-3815, doi:10.5194/acp-18-3799-2018, 2018a.

Liebmann, J., Sobanski, N., Schuladen, J., Karu, E., Hellen, H., Hakola, H., Zha, Q., Ehn, M., Riva, M., Heikkinen, L., Williams, J., Fischer, H., Lelieyeld, J., and Crowley, J. N.: Alkyl nitrates in the boreal forest: formation via the NO_3-, OH- and O_3-induced oxidation of biogenic volatile organic compounds and ambient lifetimes, Atmos. Chem. Phys., 19, 10391-10403, doi:10.5194/acp-19-10391-2019, 2019.

Liebmann, J. M., Schuster, G., Schuladen, J. B., Sobanski, N., Lelieveld, J., and Crowley, J. N.: Measurement of ambient NO_3 reactivity: Design, characterization and first deployment of a new instrument, Atmos. Meas. Tech., 10, 1241-1258, doi:10.5194/amt-2016-381, 2017.

Liebmann, J. M., Muller, J. B. A., Kubistin, D., Claude, A., Holla, R., Plaß-Dülmer, C., Lelieveld, J., and Crowley, J. N.: Direct measurements of NO_3-reactivity in and above the boundary layer of a mountain-top site: Identification of reactive trace gases and comparison with OH-reactivity, Atmos. Chem. Phys., 18, 12045-12059, doi:10.5194/acp-18-12045-2018, 2018b.

Ludwig, J., Meixner, F. X., Vogel, B., and Förstner, J.: Soil-air exchange of nitric oxide: An overview of processes, environmental factors and modeling studies, Biogeochemistry, 52, 225-257, 2001.

Marchant, A., Le Coupanec, A., Joly, C., Perthame, E., Sertour, N., Garnier, M., Godard, V., Ferquel, E., and Choumet, V.: Infection of Ixodes ricinus by Borrelia sensu lato in peri-urban forests of France, PloS One, 12, e0183543, doi:10.1371/journal.pone.0183543, 2017.

Martinez, M., Perner, D., Hackenthal, E. M., Kulzer, S., and Schutz, L.: NO_3 at Helgoland during the NORDEX campaign in October 1996, J. Geophys. Res.-Atmos., 105, 22685-22695, doi:10.1029/2000JD900255, 2000.

Feldfunktion geändert

Formatiert: Englisch (Vereinigtes Königreich)

Formatiert: Englisch (Vereinigtes Königreich)

McLaren, R., Salmon, R. A., Liggio, J., Hayden, K. L., Anlauf, K. G., and Leaitch, W. R.: Nighttime chemistry at a rural site in the Lower Fraser Valley, Atmos. Environ., 38, 5837-5848, doi:10.1016/j.atmosenv.2004.03.074, 2004.

McLaren, R., Wojtal, P., Majonis, D., McCourt, J., Halla, J. D., and Brook, J.: NO_3 radical measurements in a polluted marine environment: links to ozone formation, Atmos. Chem. Phys., 10, 4187-4206, doi:10.5194/acp-10-4187-2010, 2010.

Mermet, K., Perraudin, E., Dusanter, S., Sauvage, S., Léonardis, T., Flaud, P.-M., Bsaibes, S., Kammer, J., Michoud, V., Gratien, A., Cirtog, M., Al Ajami, M., Truong, F., Batut, S., Hecquet, C., Doussin, J.-F., Schoemaecker, C., Gros, V., Locoge, N., and Villenave, E.: Atmospheric reactivity of biogenic volatile organic compounds in a maritime pine forest during the LANDEX episode 1 field campaign, Sci. Total Environ., 756, 144129, doi:10.1016/j.scitotenv.2020.144129, 2021.

Mogensen, D., Gierens, R., Crowley, J. N., Keronen, P., Smolander, S., Sogachev, A., Nölscher, A. C., Zhou, L., Kulmala, M., Tang, M. J., Williams, J., and Boy, M.: Simulations of atmospheric OH, O_3 and NO_3 reactivities within and above the boreal forest, Atmos. Chem. Phys., 15, 3909-3932, doi:10.5194/acp-15-3909-2015, 2015.

Ng, N. L., Brown, S. S., Archibald, A. T., Atlas, E., Cohen, R. C., Crowley, J. N., Day, D. A., Donahue, N. M., Fry, J. L., Fuchs, H., Griffin, R. J., Guzman, M. I., Herrmann, H., Hodzic, A., Iinuma, Y., Jimenez, J. L., Kiendler-Scharr, A., Lee, B. H., Luecken, D. J., Mao, J., McLaren, R., Mutzel, A., Osthoff, H. D., Ouyang, B., Picquet-Varrault, B., Platt, U., Pye, H. O. T., Rudich, Y., Schwantes, R. H., Shiraiwa, M., Stutz, J., Thornton, J. A., Tilgner, A., Williams, B. J., and Zaveri, R. A.: Nitrate radicals and biogenic volatile organic compounds: oxidation, mechanisms, and organic aerosol, Atmos. Chem. Phys., 17, 2103-2162, doi:10.5194/acp-17-2103-2017, 2017.

Peräkylä, O., Vogt, M., Tikkanen, O. P., Laurila, T., Kajos, M. K., Rantala, P. A., Patokoski, J., Aalto, J., Yli-Juuti, T., Ehn, M., Sipila, M., Paasonen, P., Rissanen, M., Nieminen, T., Taipale, R., Keronen, P., Lappalainen, H. K., Ruuskanen, T. M., Rinne, J., Kerminen, V. M., Kulmala, M., Back, J., and Petaja, T.: Monoterpenes' oxidation capacity and rate over a boreal forest: temporal variation and connection to growth of newly formed particles, Boreal Environ. Res., 19, 293-310, 2014.

Pfannerstill, E. Y., Reijrink, N. G., Edtbauer, A., Ringsdorf, A., Zannoni, N., Araújo, A., Ditas, F., Holanda, B. A., Sá, M. O., Tsokankunku, A., Walter, D., Wolff, S., Lavrič, J. V., Pöhlker, C., Sörgel, M., and Williams, J.: Total OH reactivity over the Amazon rainforest: variability with temperature, wind, rain, altitude, time of day, season, and an overall budget closure, Atmos. Chem. Phys., 21, 6231-6256, doi:10.5194/acp-21-6231-2021, 2021.

Phillips, G. J., Thieser, J., Tang, M. J., Sobanski, N., Schuster, G., Fachinger, J., Drewnick, F., Borrmann, S., Bingemer, H., Lelieveld, J., and Crowley, J. N.: Estimating N_2O_5 uptake coefficients using ambient measurements of NO_3, N_2O_5, $ClNO_2$ and particle-phase nitrate, Atmos. Chem. Phys., 16, 13231-13249, doi:10.5194/acp-16-13231-2016, 2016.

Pilegaard, K.: Processes regulating nitric oxide emissions from soils, Philos. Trans. R. Soc. London, Ser. B, 368, 20130126, doi:10.1098/rstb.2013.0126, 2013.

Platt, U., and Heintz, F.: Nitrate radicals in tropospheric chemistry, Isr. J. Chem., 34, 289-300, doi:10.1002/ijch.199400033, 1994.

Pusede, S. E., Steiner, A. L., and Cohen, R. C.: Temperature and Recent Trends in the Chemistry of Continental Surface Ozone, Chem. Rev., 115, 3898-3918, doi:10.1021/cr5006815, 2015.

Romer Present, P. S., Zare, A., and Cohen, R. C.: The changing role of organic nitrates in the removal and transport of NO_x, Atmos. Chem. Phys., 20, 267-279, doi:10.5194/acp-20-267-2020, 2020.

Saathoff, H., Naumann, K. H., Riemer, N., Kamm, S., Mohler, O., Schurath, U., Vogel, H., and Vogel, B.: The loss of NO_2, HNO_3, NO_3/N_2O_5, and $HO_2/HOONO_2$ on soot aerosol: A chamber and modeling study, Geophys. Res. Lett., 28, 1957-1960, doi:10.1029/2000GL012619, 2001.

Schulze, B. C., Wallace, H. W., Flynn, J. H., Lefer, B. L., Erickson, M. H., Jobson, B. T., Dusanter, S., Griffith, S. M., Hansen, R. F., Stevens, P. S., VanReken, T., and Griffin, R. J.: Differences in BVOC oxidation and SOA formation above and below the forest canopy, Atmos. Chem. Phys., 17, 1805-1828, doi:10.5194/acp-17-1805-2017, 2017.

Smith, J. P., Solomon, S., Sanders, R. W., Miller, H. L., Perliski, L. M., Keys, J. G., and Schmeltekopf, A. L.: Atmospheric NO_3: 4. Vertical Profiles at Middle and Polar Latitudes at Sunrise, J. Geophys. Res.-Atmos., 98, 8983-8989, doi:10.1029/93JD00041, 1993.

Stull, R. B.: Stable Boundary Layer: An Introduction to Boundary Layer Meteorology, edited by: Stull, R. B., Springer Netherlands, Dordrecht, 499-543, 1988.

Stutz, J., Alicke, B., Ackermann, R., Geyer, A., White, A., and Williams, E.: Vertical profiles of NO_3, N_2O_5, O_3, and NO_X in the nocturnal boundary layer: 1. Observations during the Texas Air Quality Study 2000 J. Geophys. Res.-Atmos., 109, D12306, doi:10.1029/2003JD004209, 2004.

Vermeuel, M. P., Novak, G. A., Kilgour, D. B., Claflin, M. S., Lerner, B. M., Trowbridge, A. M., Thom, J., Cleary, P. A., Desai, A. R., and Bertram, T. H.: Observations of biogenic volatile organic compounds over a mixed temperate forest during the summer to autumn transition, Atmos. Chem. Phys., 23, 4123-4148, doi:10.5194/acp-23-4123-2023, 2023.

von Friedeburg, C., Wagner, T., Geyer, A., Kaiser, N., Vogel, B., Vogel, H., and Platt, U.: Derivation of tropospheric NO_3 profiles using off-axis differential optical absorption spectroscopy measurements during sunrise and comparison with simulations, J. Geophys. Res.-Atmos., 107, 4168, doi:10.1029/2001JD000481, 2002.

Wayne, R. P., Barnes, I., Biggs, P., Burrows, J. P., Canosa-Mas, C. E., Hjorth, J., Le Bras, G., Moortgat, G. K., Perner, D., Poulet, G., Restelli, G., and Sidebottom, H.: The nitrate radical: Physics, chemistry, and the atmosphere, Atmos. Env. A, 25A, 1-206, doi:10.1016/0960-1686(91)90192-A, 1991.

Yan, Y. H., Wang, S. S., Zhu, J., Guo, Y. L., Tang, G. Q., Liu, B. X., An, X. X., Wang, Y. S., and Zhou, B.: Vertically increased NO_3 radical in the nocturnal boundary layer, Sci. Total Environ., 763, 142969, doi:10.1016/j.scitotenv.2020.142969, 2021.

Figures

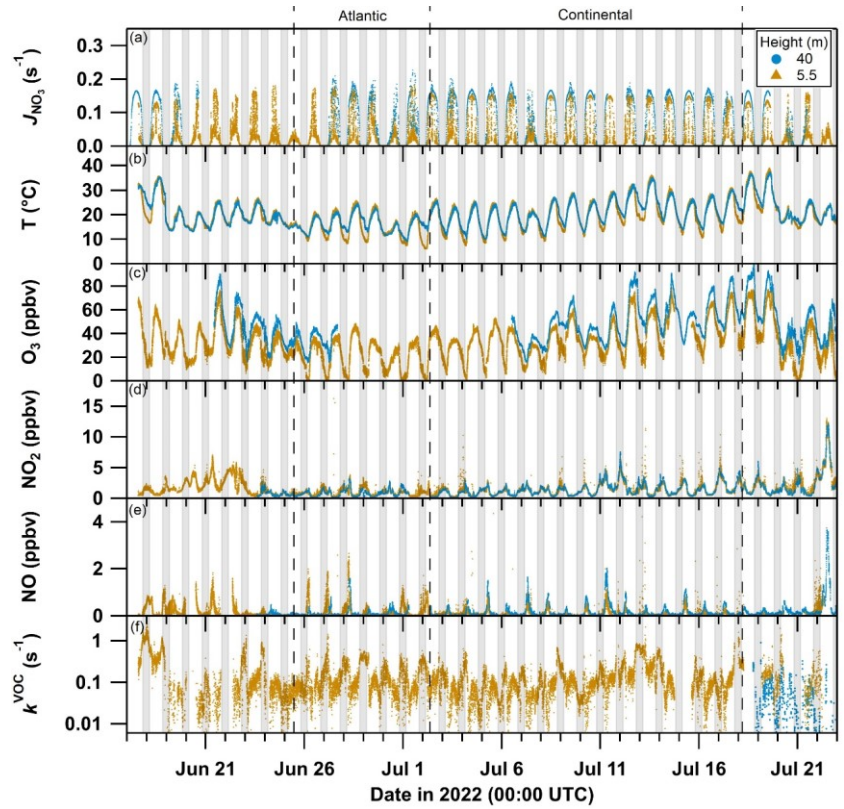

Figure 1: Time series of NO_3 photolysis ~~rates~~ frequencies ($J_{NO_3}^{NO_3}$, panel a), temperature (T, panel b), ozone (O_3, panel c), nitrogen dioxide (NO_2, panel d), nitric oxide (NO, panel e) and VOC-induced NO_3 reactivity (k^{VOC}, panel f) sampled at 5.5 m (orange triangles, 3.2 m and 5 m for NO and T, respectively) and 40 m (blue circles) above ground level. Major and minor ticks on the x-axis represent 00:00 UTC of the corresponding date. Dashed lines separate periods with air of Atlantic and continental origin. Nighttime periods are grey-shaded.

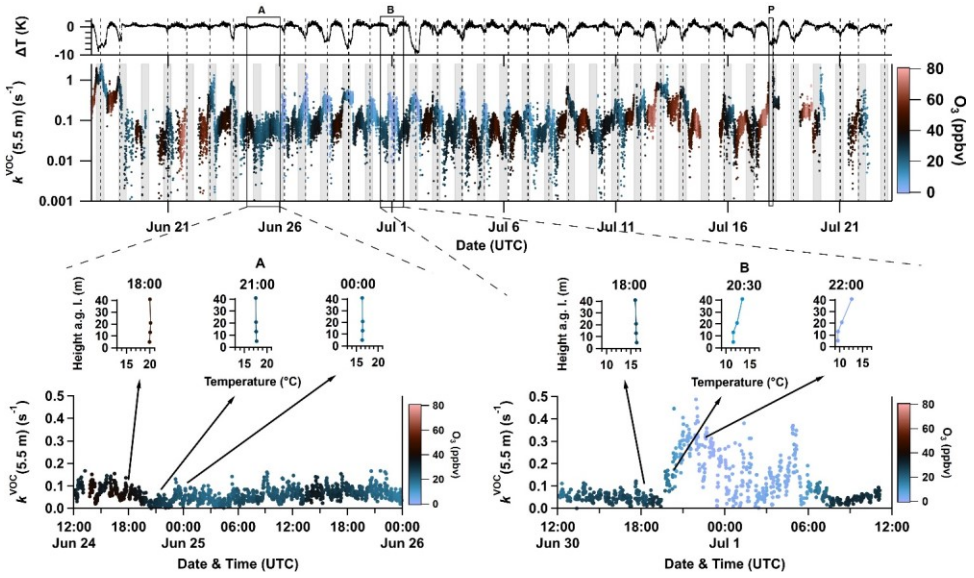

Figure 2: Time series of k^{VOC} (second panel, logarithmic scale) near ground level (5.5 m) coloured by O_3 mixing ratios measured at the same height (colour scale on the right). Nighttime periods are grey-shaded. The difference between temperatures measured at 5 m and 41 m (ΔT) is plotted in the first panel. Temperature inversions are marked by dashed, vertical lines. Periods A (lower left panel) and B (lower right panel) exemplify daytime-nighttime transitions both with (right) and without (left) clear temperature inversions, with NO_3 reactivity plotted along with temperature profiles at selected times. A vertical profile of k^{VOC} was measured in period P (see section 3.5).

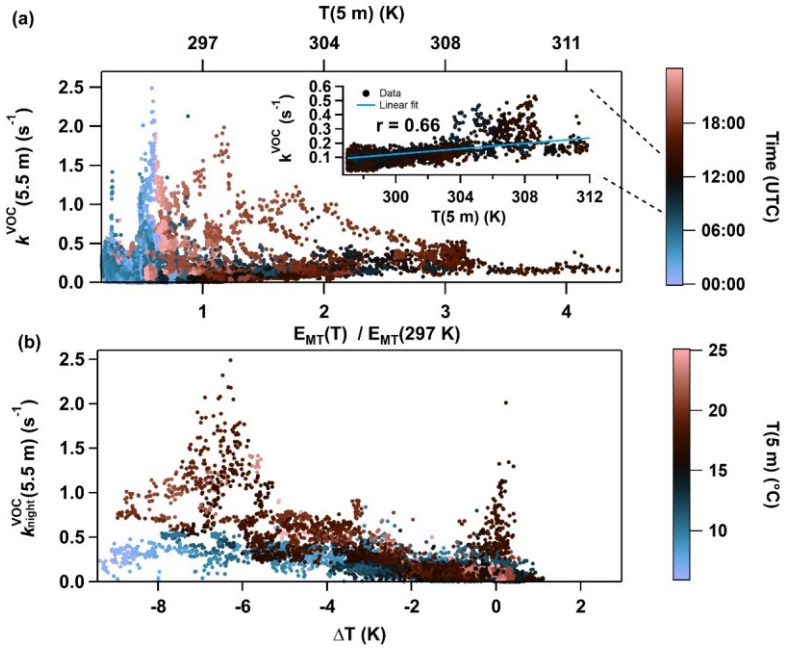

Figure 3: (a) NO_3 reactivity at 5.5 m ($k^{VOC}(5.5\,m)$) plotted against the ~~calculated~~ expected change in the monoterpene emission factor (E_{MT}) relative to 297 K using $E_{MT} \propto \exp(0.1K^{-1}(T - 297K))$ (Guenther et al., 1993). Data points are coloured according to time of the day (UTC) with night/morning (blue), daytime (black~~green~~) and afternoon/night (red~~orange~~). The inset shows $k^{VOC}(5.5\,m)$ between 10:00 and 14:00 UTC plotted against air temperature (5 m). Linear regression (blue solid line) yields a Pearson correlation coefficient (r) of 0.66. (b) Nocturnal ground-level NO_3 reactivity k^{VOC}_{night}(5.5 m) plotted versus the temperature difference (ΔT) between 41 m and 5 m. The data points are coloured according to the ground-level temperature T(5 m).

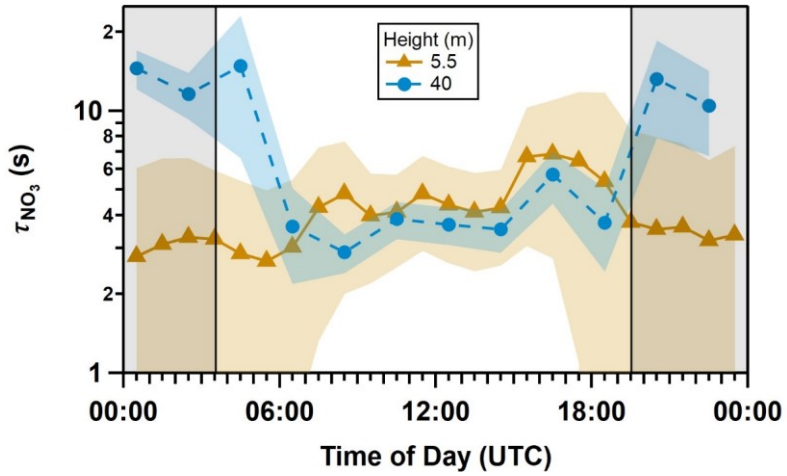

Figure 4: Mean diel cycle of overall NO_3 lifetime ($\tau_{NO_3}^{NO_3}$) calculated from Eq. (2) at 5.5 m (dark orange triangles~~points~~ with solid line, June 17 – July 23) and 40 m (blue circles~~points~~ with dashed line, every 2h, July 18 – July 23). Shaded areas represent the standard deviation (1σ). The nighttime period (19:30 to 03:30 UTC) is shaded grey.

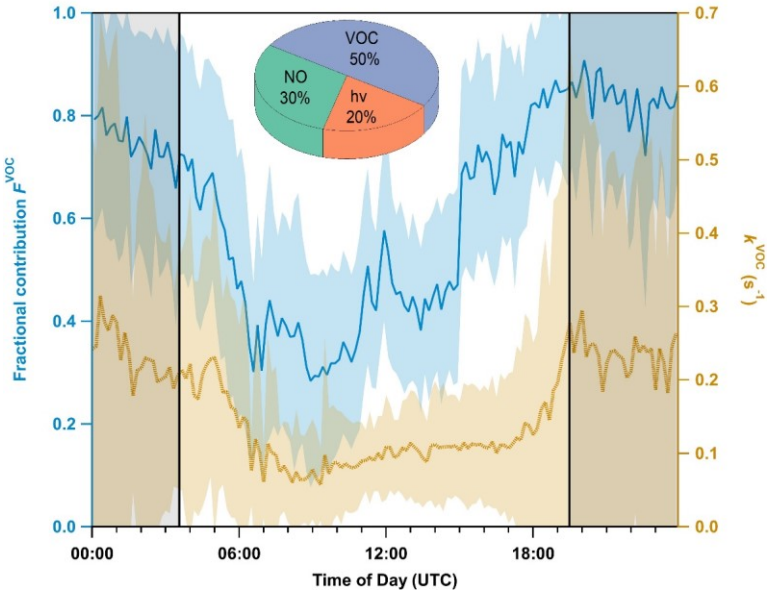

Figure 5: Mean diel profiles (10 min averages, June 17 – July 23) of VOC-induced NO_3 reactivity (k^{VOC}, right y-axis) at 5.5 m along with its fractional contribution (F^{VOC}, left y-axis) to the overall NO_3 loss. Shaded areas represent the standard deviation (1σ). The nighttime period is grey-shaded and separated by black solid lines. The pie chart shows the fractional contribution of each process in Eq. (1) to the overall NO_3 loss term during the day.

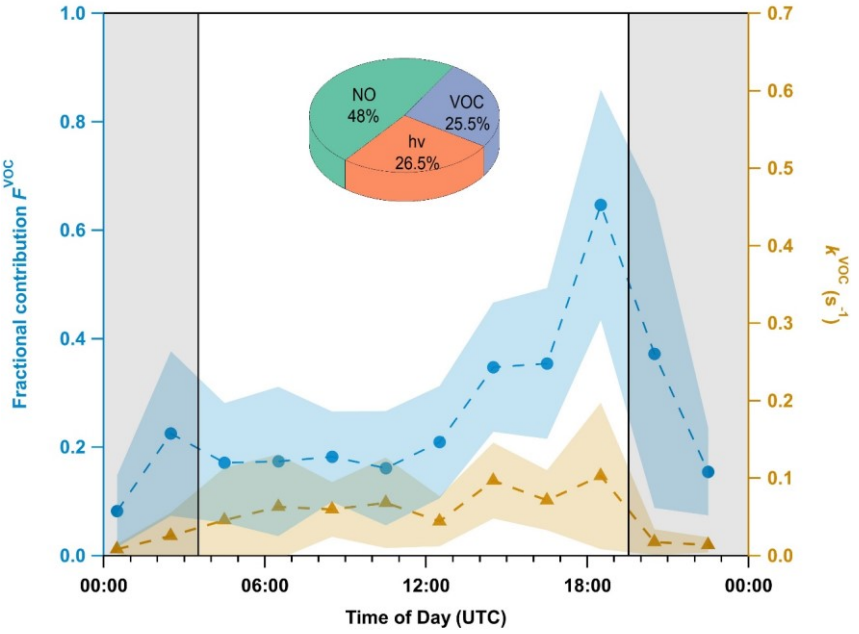

650

Figure 6: Mean diel profiles (1h averages, every two hours, July 18 – July 23) of VOC-induced NO_3 reactivity (k^{VOC}, orange triangles) at 40 m along with its fractional contribution (F^{VOC}, blue ~~line~~circles) to the overall NO_3 loss. Shaded areas represent the standard deviation (1σ). The nighttime period is grey-shaded. The pie chart shows the fractional contribution of each process in Eq. (1) to the overall NO_3 loss term during the day.

655

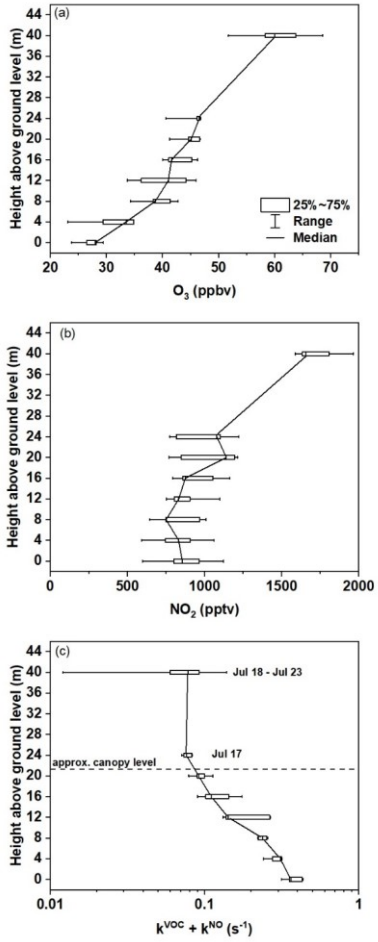

660

Figure 7: Box-and-whisker plots (full range, 25th, 50th and 75th percentiles) of vertical profiles of (a) O_3 (b) NO_2 and (c) total gas-phase NO_3 reactivity ($k^{VOC} + k^{+NO}$) measured during the temperature-inverted night of Jul 17 to Jul 18 between 20:00 and 00:00 UTC. NO_3 reactivities measured on top of the tower (40 m) during the nights between July 18 to July 23 are also shown.

Formatiert: Schriftart: Kursiv

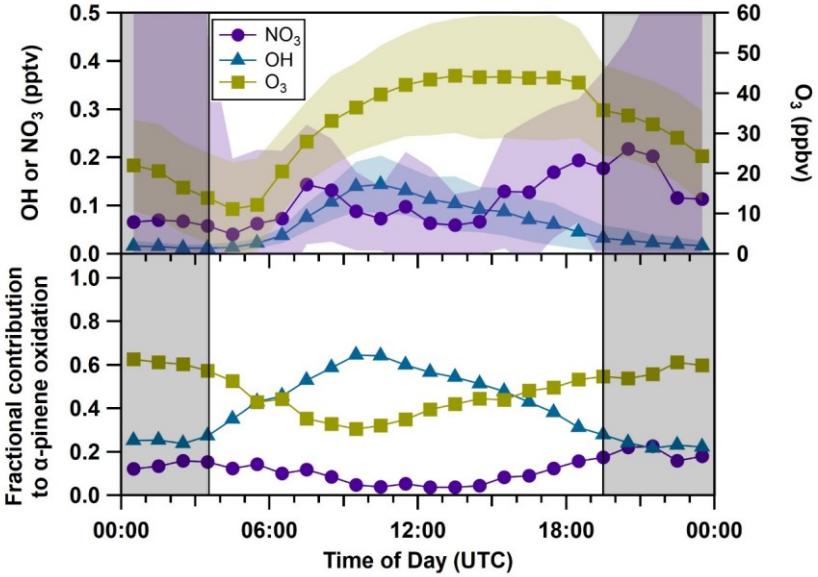

Figure 8: Campaign-averaged median ~~(circles)~~ diel profiles (1h) of the oxidants (upper panel) $[NO_3]_{ss}$ (violet circles), OH (blue triangles) and O_3 (dark yellow squares) and their contribution to the overall ~~oxidative~~ loss rate coefficient of α-pinene according to Eq. (4) close to the ground (lower panel). The nighttime period is grey-shaded. Shaded areas represent the standard deviation (1σ).

Supplement

S1 Wind rose

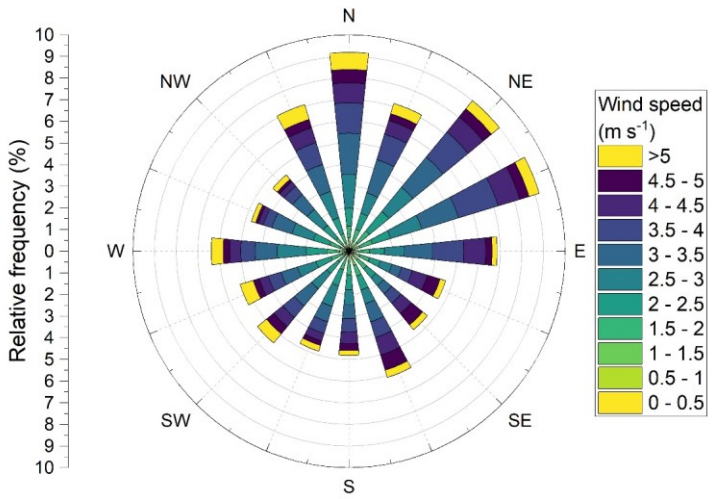

Figure S1: Wind rose coloured according to wind speed as measured at a height of 40 m during the ACROSS campaign.

S2 NO_3 reactivity measurements above and below the canopy

Figure S2 shows the time-series of k^{VOC} measured at 5.5 m (every odd hour) and at 40 m (every even hour) between July 18 and July 23. Note that the data coverage of k^{VOC}(5.5 m) is reduced due to missing NO measurements. During the daytime period of July 21, k_{day}^{VOC} is about (0.05 ± 0.03) s^{-1} at both heights. From ca. 17:00 UTC on, k^{VOC}(5.5 m) and k^{VOC}(40 m) diverge with an increase in both the magnitude and variability of the former and a continuous decrease in the latter to the instrument LOD of 0.006 s^{-1} at ~22:30 UTC. On this night, there was a moderate temperature inversion (ΔT = -2.9 K, Fig. 2) and the inlet at 40 m (ca. 20 m above canopy level) was thus effectively decoupled from any sources of biogenic emissions, explaining the low reactivity at this height. Furthermore, contrary to the daytime when the variability in k^{VOC} was similar at both heights, at night k^{VOC} (40 m) is less affected by short-term fluctuations, presumably a result of enhanced mixing above canopy. It is also observed that k^{VOC}(5.5 m) and k^{VOC}(40 m) show a similar diel profile on July 19-20. However, k_{day}^{VOC} between the two heights differ by a factor of 2 and a weaker nocturnal gradient in k_{night}^{VOC} (only a factor of 4) occurs. The latter presumably results from a weaker, less stable temperature inversion (ΔT ≈ -0.5 K, Fig. 2) during that night.

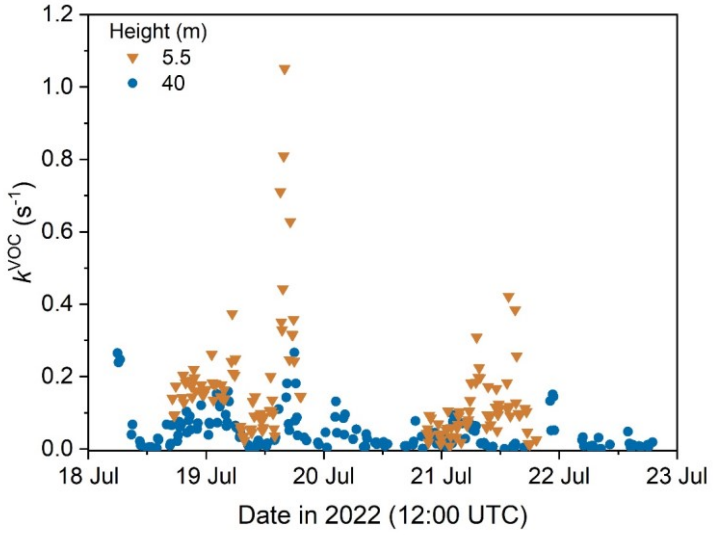

Figure S2: Time series of k^{VOC} (10 min averages) at 5.5 m (dark orange ~~dots~~triangles) and 40 m (blue dots) between July 18 and July 23 during the ACROSS campaign. Major and minor ticks on the x-axis represent 12:00 and 00:00 UTC, respectively.

S3 Impact of OH, XO_2 and heterogeneous reactions of N_2O_5 on NO_3 loss

A chemical ionization mass spectrometer (CIMS) measured the sum of peroxy radicals (XO_2 = RO_2 + HO_2) as well as OH radicals ca. 3 m above ground level via their conversion to sulphuric acid (H_2SO_4) by sulphur dioxide (SO_2). Nitrate ions (NO_3^-) serve as ionization agent. The associated measurement uncertainty of XO_2 is ca. 30 % (2σ) with an LOD of 2 x 10^6 molecule cm^{-3} (4 min). A detailed description of the instrument can be found in Kukui et al. (2008). IUPAC-recommended rate coefficients (IUPAC, 2024) were used to derive pseudo first-order NO_3 loss rate coefficients. In case of XO_2, the reaction rate coefficient of RO_2 was set to the value of HO_2 (4 x 10^{-12} cm^3 $molecule^{-1}$ s^{-1}), since isoprene-derived RO_2 are suspected to be a factor of two more reactive (4.6 x 10^{-12} cm^3 $molecule^{-1}$ s^{-1}) towards NO_3 (Dewald et al., 2020) than for instance ethyl peroxy radicals. Losses of NO_3 via its reaction with OH, HO_2 and RO_2 (Fig. S3) were, with a campaign-averaged mean contribution of 0.003 s^{-1}, found to be insignificant compared to photolysis and VOC-induced losses.

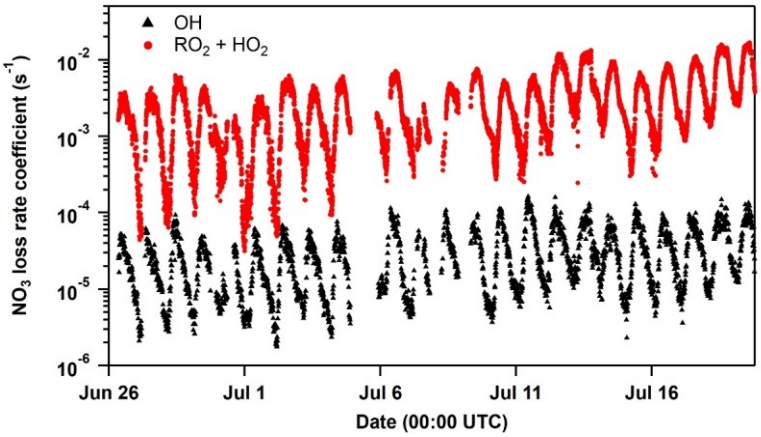

Figure S3: Time series of pseudo first-order NO_3 loss rate coefficients from OH (black) and RO_2 + HO_2 (red).

In addition, neither direct nor indirect heterogeneous losses (via N_2O_5) of NO_3 are expected to contribute significantly to the NO_3 loss term. Assuming a large uptake coefficient γ of 0.03 for N_2O_5 (featuring a mean molecular velocity c of 26233 cm s^{-1} at 298 K) and a surface area (A_S) of 1.5 x 10^{-6} cm^2 cm^{-3} in a semi-rural environment (Phillips et al., 2016) together with the equilibrium constant (K_{eq}) for reactions R3 and R4 of 2.8 x 10^{-11} cm^3 $molecule^{-1}$ at 298 K (IUPAC, 2024) would result in a k_{het} = $0.25\gamma c A_s K_{eq}[NO_2]$ = 4 x 10^{-4} s^{-1} in case of 2 ppbv NO_2 at noon (see Fig. 1). Heterogeneous uptake is thus only of very minor importance below the canopy.

S4 NO_3 loss rate coefficientss (sum, NO, photolysis) above and below the canopy between July 18 and July 23

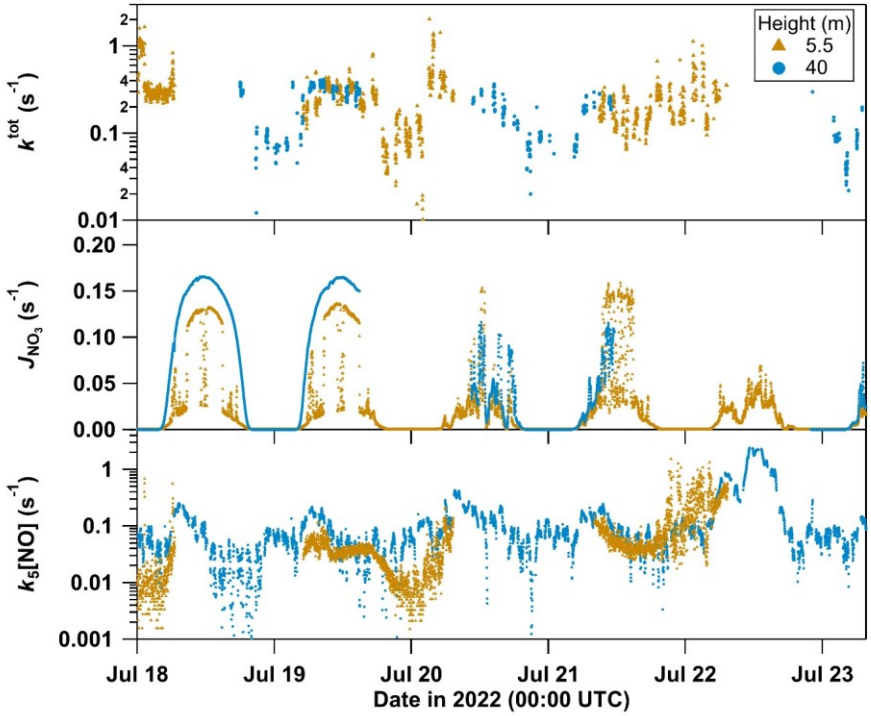

Figure S4: Time series of $k_5[NO]$, ~~J^{NO_3}~~ J_{NO_3} as well as ~~kL^{totNO_3}~~ at 5.5 m (dark orange dots) and 40 m (blue dots) between July 18 and July 23 during the ACROSS campaign. Major and minor ticks on the x-axis represent 00:00 UTC.

S5 NO_3 photolysis frequencies~~rates~~ above and below the canopy

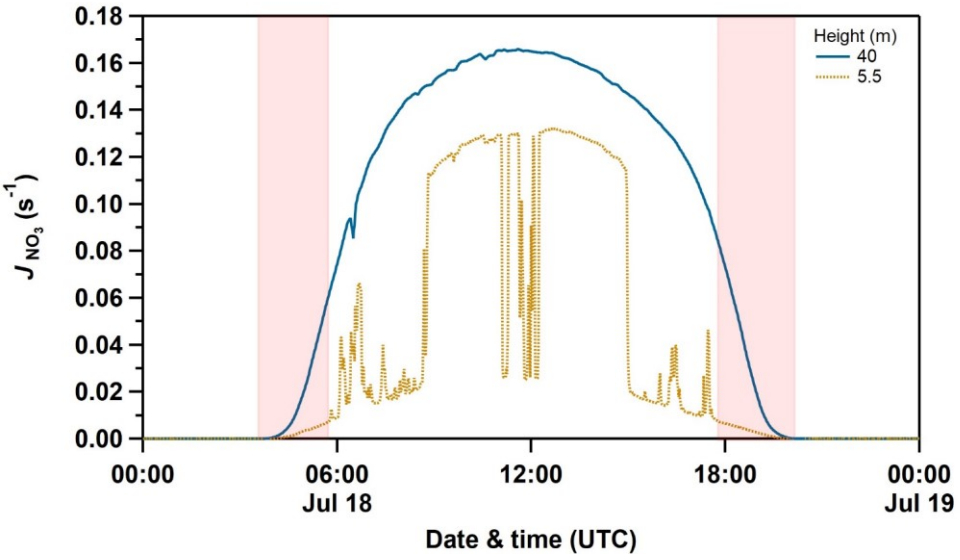

Figure S5: Exemplary diel profile of NO_3 photolysis frequencies~~rates~~ ($J_{NO_3}^{NO_3^-}$) measured in the clearing below the canopy (orange line, 5.5 m) versus those measured on top of the tower above the canopy (blue line, 40 m) during the ACROSS campaign on a clear day. The red shades mark periods in the early morning and the late afternoon when only diffuse sunlight reached the spectral radiometer below the canopy. As a consequence, $J_{NO_3}^{NO_3^-}$(5.5 m) was on average a factor of 12.5 lower than $J_{NO_3}^{NO_3^-}$(40 m) during these periods.

S6 Fractional contributions of OH, O_3 and NO_3 to oxidation of other monoterpenes

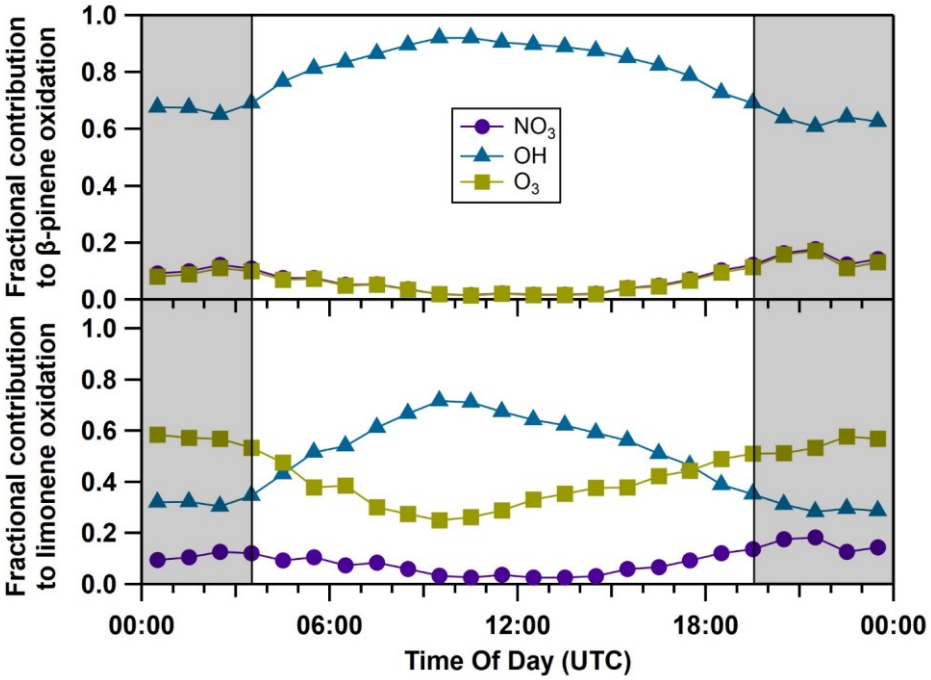

Figure S6: Median diel cycles (1h, circles) of fractional contributions of NO_3 (violet), OH (green) and O_3 (dark yellow) to the oxidation of β-pinene (upper panel) and limonene (lower panel) during the ACROSS campaign. The nighttime period is grey-shaded.

References

Dewald, P., Liebmann, J. M., Friedrich, N., Shenolikar, J., Schuladen, J., Rohrer, F., Reimer, D., Tillmann, R., Novelli, A., Cho, C. M., Xu, K. M., Holzinger, R., Bernard, F., Zhou, L., Mellouki, W., Brown, S. S., Fuchs, H., Lelieveld, J., and Crowley, J. N.: Evolution of NO_3 reactivity during the oxidation of isoprene, Atmos. Chem. Phys., 20, 10459-10475, doi:10.5194/acp-20-10459-2020, 2020.

IUPAC: Task Group on Atmospheric Chemical Kinetic Data Evaluation, edited by: Ammann, M., Cox, R.A., Crowley, J.N., Herrmann, H., Jenkin, M.E., McNeill, V.F., Mellouki, A., Rossi, M. J., Troe, J. and Wallington, T. J.: https://iupac.aeris-data.fr/en/home-english/, access: 29 January, 2024.

Kukui, A., Ancellet, G., and Le Bras, G.: Chemical ionisation mass spectrometer for measurements of OH and Peroxy radical concentrations in moderately polluted atmospheres, J. Atmos. Chem., 61, 133-154, doi:10.1007/s10874-009-9130-9, 2008.

Phillips, G. J., Thieser, J., Tang, M. J., Sobanski, N., Schuster, G., Fachinger, J., Drewnick, F., Borrmann, S., Bingemer, H., Lelieveld, J., and Crowley, J. N.: Estimating N_2O_5 uptake coefficients using ambient measurements of NO_3, N_2O_5, $ClNO_2$ and particle-phase nitrate, Atmos. Chem. Phys., 16, 13231-13249, doi:10.5194/acp-16-13231-2016, 2016.

Feldfunktion geändert